EFFECT OF INFILL ANGLE ON TENSILE STRENGTH OF SOLID 3D-PRINTED CARBON FIBER REINFORCED ACRYLONITRILE BUTADIENE STYRENE (ABS)

A THESIS

SUBMITTED TO THE GRADUATE SCHOOL

IN PARTIAL FIFILLMENT OF THE REQUIREMENTS

FOR THE DEGREE

MASTER OF ARTS - TECHNOLOGY EDUCATION

BY

CALE RAUCH

DR. JIM FLOWERS - ADVISOR

BALL STATE UNIVERSITY

MUNCIE, INDIANA

MAY, 2018

Acknowledgments

I would like to thank Dr. Jim Flowers who was the committee head, mentor, and advisor for the entire process of this study. I could not have done this study without him, and I will appreciate all his efforts put into my entire academic career for eternity.

I would like to thank my life partner, Amanda Wilhelm, who worked hard to help me keep my sanity throughout this study.

I would like to thank my father, Don Rauch, who continued to assure me that I am capable of anything, and that I would get through this study.

I would like to thank Dr. Annette Rose and Dr. Renmei Xu for their commitment and valuable time taken to be instrumental parts of the committee for this study.

Table of Contents

Chapter 1: Introduction

Market trends show that between the years of 2009 and 2013, 3D-printer sales and services revenue doubled and continues to grow rapidly (Park, 2014). Although technologies such as these "were originally intended exclusively for (heavy) industrial use, the constant decrease in cost has put them within reach of [subject matter experts] SMEs and individual entrepreneurs" (Rayna & Striukova, 2016, p. 215). In addition, consumer markets also show a growing trend in general sales in stores such as Staples and Walmart (Rayna & Striukova, 2016, p. 215). Online outlets such as 3DX-Tech (2017a), Stratasys (2017), and Makerbot (2017) have been selling proprietary materials of their own ingredients while Amazon, Ebay, and other vendors supply third-party materials and 3D-printing services to general consumers and major manufacturers in the industry (Rayna & Striukova, 2016, pp. 215-216). Market trend predictions for 2018 suggest that 25% of the worlds' manufacturers will introduce some kind of 3D-printer; high-quality 3D-printers will be available for less than $2,000 (Park, 2014). With 3D-printing becoming more commercially available to the general public, there is a clear need to have the ability to produce items which are expected to exhibit certain mechanical properties. Consumers would appreciate more information about mechanical properties of filaments available from producers and third-party distributors.

According to Novakova and Kuric (2012), Fused Deposition Modeling (FDM) – a subset of 3D-printing – "was developed by Stratasys in Eden Prairie, Minnesota; in this process, a plastic or wax material is extruded through a nozzle that traces the part's cross-sectional geometry layer by layer" (p. 24). As the model is grown, each layer consists of extruded strands lined up and welded next to one-another. Extruded strands make up one or more layers of the

shell of an object, as well as its internal structure or *infill.* Changes can be made to the mechanical nature of the product being 3D-printed through software settings and material choice.

Tensile strength is an important material property for 3D-printed parts because some may be required to withstand such forces. To experiment with the tensile strength of FDM parts made out of acrylonitrile butadiene styrene (ABS), infill orientations have been altered by researchers such as Torrado, Roberson, and Wicker (2014) and Hossain, Ramos, Espalin, Perez, and Wicker (2013); they found that as strands are laid more in-line with the direction of applied forces, tensile strength increases; additionally, perpendicular orientations (e.g., one layer being extruded at a -45 degree angle and the successive layer being laid at +45 degrees) give better tensile results than those which are not (e.g., a +30 degree orientation layer followed by a -60 degree angle). Furthermore, carbon fibers do not adhere well to ABS, and researchers such as Li and Zhang (2009) tried improving this adhesion through applying surface-additives to the fibers such as nitric acid (HNO_3) (p. 538).

Ning, Wong, Qiu, Wei, and Wang (2015) noted that many common 3D-printing materials are for the creation of non-structural models intended to illustrate the form and components of a new design rather than to serve a load-bearing requirement; however, this idea does not allow for the mechanical ability these components could possess with the specific designs and materials. These restrictions promote a "critical need to improve the strength of FDM-fabricated pure thermoplastic parts to overcome the limitations" (Ning et al. 2015, p. 370). Thakur (2017) proclaims that "the quality of a product is often measured in terms of strength and accuracy. The quality attributes like strength and accuracy is [*sic*] essential for the success

of any [Rapid Prototyping] RP process" (Abstract, p. iv). Rapid prototyping (RP) refers to "techniques used to quickly fabricate physical models" (Schaefermeier et al., 2009, p. 52). Furthermore, the "strength of RP parts depends on various factors like infill percentage, infill orientation, temperature (build-platform temperature and extruder temperature), infill patterns etc." (Thakur, 2017, p. 10). Infill refers to 3D-printed extruded strands of plastic filament laid inside the area of shell strands (sometimes in a specified pattern or angle) as designated by the software that controls the 3D-printer.

In an attempt to improve tensile strength of 3D-printed models, carbon fibers have been added to consumer-available ABS. Claims are made by companies such as 3DX-Tech (2017g) that carbon fiber reinforced (CFR) ABS produces a higher tensile strength than that of non-reinforced ABS (see Appendix-B & D). Tekinalp et al. (n.d.) report that "the tensile strength and modulus of 3D-printed samples increased ~115% and ~700%, respectively. 3D-printer yielded samples with very high fiber orientation in printing direction (up to 91.5%)" (Abstract section); therefore, carbon fibers within a material are anticipated to increase the tensile strength of models due to their alignment with the strands of plastic being laid (p. 149). A sufficient amount of information about tensile strength differences based on reinforcements added to solid 3D-printed models grown in specified infill orientations has not been produced. Manufacturers do not make mention of which infill orientation is best for strands to be laid in terms of tensile strength for a model being 3D-printed with CFR ABS.

Purpose and Research Questions

The purpose of this study is to determine the effects of infill angle and two materials on tensile strength for parts made by 3D-printing. The study entails an experimental approach with

a purpose of understanding how the tensile strength of solid 3D-printed ABS and CFR ABS samples differ if their infill angles (or strand orientations) to the longitudinal axis (the load-bearing direction) are changed. Preliminary testing has shown that the orientation of the direction of interior strands with respect to the longitudinal axis of a tensile-test model impact tensile-testing results. A 3D-printer lays each infill angle by-layer. Therefore, if a sample was grown with an infill angle of ±45 degrees, the first layer would be strands laid at +45 degrees to the longitudinal axis, and then the second layer would be -45 degrees, continuing in succession until the model is complete. Therefore, a tensile specimen with an infill orientation of ±15 degrees is anticipated to have different results than a specimen with strands laid at ±75 degrees. Angular degrees used in the current study include ±15, 30, 45, 60, 75, and 90 (0/90). Each of these - except ±45 and 0/90 - has different vectors (i.e., a quantity that is specified by both a length and a direction, Walker, 2014 p. 114), which were anticipated to change the tensile strength results. It is hypothesized that a greater total vector quantity in the direction of stress would likely result in a greater strength in that direction.

The research questions that guide this study include:

- How does infill angle affect the tensile strength of solid 3D-printed ABS samples?
- How does infill angle affect the tensile strength of solid 3D-printed CFR ABS samples?
- What differences exist in tensile strength of ABS and CFR ABS at a given infill orientation?

Definition of Terms

This listing features key terms and their definitions as they apply throughout the content of the current study (listed alphabetically).

- 3D-Printing / Fused Filament Fabrication: "refers to a class of technologies for the direct fabrication of physical products from 3D computer aided design (CAD) model by a layered manufacturing process" (Huang, Zhang, Sabbaghi, Dasgupta, & Epstein, 2012, p. 2).
- Acrylonitrile Butadiene Styrene (ABS) $(C_8H_8 \cdot C_4H_6 \cdot C_3H_3N)_n$: a terpolymer and a "rubber-toughened thermoplastic" consisting of a "blend of Styrene-acrylonitrile copolymer and polybutadiene" (Sivaraman, Chandrasekhar, Mishra, Chakraborta, & Varghese, 2006, p. 562).
- Anisotropy: "exhibiting different mechanical properties in different directions" (Depaula et al., 2005, p. 296)
- Carbon Fiber: "a fiber containing at least 92 weight (wt) percent (%) anisotropic carbon" (Huang, 2009, p. 2369). Additionally, these fibers generally have excellent tensile properties (Lee & Witting, 2016, p. 1).
- Composite: a material that consists "of two or more different materials that form regions large enough to be regarded as continua and which are usually firmly bonded together at the interface" (Hashin, 1983, p. 481). "One of the materials that ensure the connection is known as the matrix and the other which imparts resistance is called the reinforcement. The reinforcement presents itself generally in the form of particles, short fibres [*sic*] or long fibres [*sic*]" (Kumar, Ananthaprasad, & Krishna, 2015).
- Elastometer: a device attached to a tensile-testing specimen that determines elastic elongation measurements in the direction which force being applied as the specimen is stretched (ASTM D 638 – 02, p. 48 & 52).

- Extrusion: process of continuously forcing a thermoplastic molten material (the extrudate) to flow through a die of a specified shape and size.
- Fiber: "any particle with a length >5 μm and a length-to-diameter ratio of >3:1" (SAT LLC, 2006).
- Fiber-Loading: "percentage (wt%) of fiber [in this case carbon fiber] present in the composite" (Panda, 2012, p. 6).
- Filament: an individual indefinite "fiber produced from a liquid bath as by extrusion through a small orifice" (Horton, 1989, p. 7).
- Glass Transition Temperature: "the temperature below which the material behaves like a glass and above which the material is rubberlike and soft" (Ferry, 1980, as cited in Gururaja et al., 1985, p. 485).
- Hygroscopic: "absorbs water from the surrounding environment" (Goldfein & Slavin, 2015, Preservation, para. 1).
- Infill: 3D-printed extruded strands of plastic filament laid inside the area of shell strands (sometimes in a specified pattern or angle) as designated by software.
- Infill Angle/Orientation: the predominate direction in which 3D-printer extruded strands are laid in relation to the longitudinal axis of the model where it is situated along the x-axis of the build-platform.
- Load-cell: part of a stress-testing machine (in this case a tensile-tester) which withstands the forces of the object being tested.
- Magnitude: see Vector.
- Matrix: see Composite.

- Melt Flow Index: "measures the rate of extrusion of thermoplastics through an orifice at a prescribed temperature to provide a means of measuring flow of a melted material" (ASTM, 2013).
- Modulus (of elasticity): an elasticity measurement which "is determined [during a tensile-test] from the slope of the linear portion of the stress-strain curve"; determined with an elastometer. (ASTM D 638 – 02, 2012, p. 52 & 53). "The ratio of stress (nominal) to corresponding strain below the proportional limit of a material" (p. 56).
- Monomer: "a molecule of simple structure and low molecular weight [mass] that is capable of coming with a number of like or unlike molecules" (Martin, Graff, Gross, Hall, & Mast, 2005, Background of the Invention, para. 5).
    - Polymer: "organic compound having repeating units of similar or different monomers" (Wang & Essner, 2002, p. 4).
    - Copolymer: …having repeating units of two monomers.
    - Terpolymer: …having repeating units of three monomers.
- Rapid Prototyping (RP): "techniques used to quickly fabricate physical models" (Schaefermeier et al., 2009, p. 52).
- Shell Strands: 3D-printed perimeter strands laid before infill is added. These strands typically give a model its shape due to acting as the outer most strands.
- Tensile Strength: "the maximum tensile stress (nominal) sustained by the specimen during a tension test". (ASTM D 638 – 02, 2012, p. 57).

- Thermoplastic: “a material that softens when heated, hardens when cooled” (Merrill & Sagar, 1995, p. 3). Thermoplastics can repeat this process many times without severely compromising the materials original integrity shown prior to temperature changes.
- Vector: “a quantity that is specified by both a length and a direction; the length of a vector is referred to as its magnitude” (Walker, 2014 p. 114).
- Yield Point: “the first point on the stress-strain curve at which an increase in strain occurs without an increase in stress” (ASTM D 638 – 02, p. 58).

Chapter 2: Review of the Literature

Several key areas of this research have been discussed in related literature, including: fused deposition modeling (FDM), ABS with discussion of tensile strength, carbon fiber reinforcement in ABS with discussion of tensile strength, manufacturers of CFR ABS, and tensile strength differences based on orientation of 3D-printed strands.

Fused Deposition Modeling (FDM)

Brooks, Kinsley, and Owens (2014) report that FDM was first brought to use and began turning into what we know of as FDM today in the 1980s by S. Scott Crump who cofounded Stratasys. Since the patent for FDM has expired, the cost of commercial 3D-printers has declined rapidly as more companies and open-source markets pick up the idea of making a machine or material for the machine (p. 273-274). These researchers go on to conclude that since FDMs development, "companies are now beginning to realize the possibilities of using this technology within their business model for competitive advantage" (p. 277). For instance, companies can use a wide variety of materials to serve a wider variety of customers.

Bhargava, Bhargava, and Jangid (2014) note that FDM processes can create a wide variety of parts such as "prototyping, tooling, and manufactured goods" from a variety of materials including "paper, nylon, wax, resins, metals and ceramics". The researchers go on to conclude that "A wide range of industries can benefit from FDM and these include automotive, aerospace, biomedical, consumer, electrical and electronic products" (p. 4). This advantage comes from the fact that FDM is "unlike some additive fabrication processes, FDM requires no special facilities or ventilation and involves no harmful chemicals and byproducts" (p. 4).

Additionally, parts made through FDM are ready for use with “very little delay and labor” while also eliminating components like tooling and other costly items (p. 1.)

“The term additive manufacturing (AM) refers to the production technologies that create objects through a sequential layering process” (Fudali, Witkowski, & Wydrzyński, 2013, p. 36). Some of these technologies include Fused Filament Fabrication (FFF), also known as fused deposition modeling (FDM), and 3D-printing which “refers to a class of technologies for the direct fabrication of physical products from 3D computer aided design (CAD) model by a layered manufacturing process” (Huang, et al., 2012, p. 2). A virtual 3D-model of a product to be 3D-printed entails the use of AM. Software is used to plot consecutive horizontal cross sections, and each cross section is treated as a 2D geometrical shape of a set height.

A 3D-printer then creates (or grows) models one layer at a time by extrusion of a thin strand of a semi-molten thermoplastic, often ABS, through a heat-resistive nozzle/orifice (Berman, 2007; Novakova-Marcincinova & Kuric, 2012). This process uses a spooled filament of thermoplastic, typically .07 inch (1.75 mm) or .12 inch (3 mm) in diameter, to construct the horizontal thin slice of the model generated by software. Beginning with a base layer, the filament is heated to a specified thermal degree and extruded through a small nozzle (with a circular orifice typically .0079 inch (.2 mm) to .28 inch (.7 mm) in diameter) to lay down a strand of plastic onto a build-platform to which the first layer of plastic temporarily bonds. Additional paths are made until the entire layer has been built. Each layer of the model typically has strands laid down along the perimeter called shell strands. If the model is specified to be built with a solid interior, interior regions are often made up of strands laid down at a set angle (such as +45° to the x-axis of the build-platform, which runs left and right) (Novakova-Marcincinova &

Kuric, 2012). When the machine moves to the next successive layer through a process of the build-platform moving down by the amount designated by individual layer thickness, the next layer by default is grown perpendicular to and on top of the previous layer (such as - 45° to the x-axis), where it coheres. In some models, interior zones are not solid but have honeycomb or other geometrical orientations of material to decrease material use, model cost, build time, or model density.

Where there are substantial overhangs of 3D-printed material, or an upper layer is insufficiently supported in some regions by the layer beneath it, supports may be built (sometimes with dissolvable or otherwise easily removable materials). Where there is inadequate adhesion to the build-platform, a special set of base layers sometimes called a raft or a brim can be built (as a new platform for the model to be built upon) to keep the model from becoming dislodged from the base during manufacture. After the model is grown, rafts, brims, and supports are removed. As this extrusion process takes place, the material traces the CAD model's cross-sectional geometry layer-by-layer, eventually becoming the finished product (Novakova-Marcincinova & Kuric, 2012).

Acrylonitrile Butadiene Styrene (ABS)

$$(C_8H_8 \cdot C_4H_6 \cdot C_3H_3N)_n$$

According to Olivera, Muralidhara, Venkatesh, Gopalakrishna, and Vivek, (2016), "the origins of ABS plastic (chemical formula shown above) can be traced back to mid-1940s" (p. 3658). The original formulation did not include butadiene (C_4H_6) which caused issues within the copolymer acrylonitrile-styrene. Once adding this rubber monomer and creating the terpolymer we now know as ABS, bulletproof armor was produced in World War II because of its high

resistance to impact and “low thermoplastic flow properties” (p. 3658). “ABS polymers exhibit high toughness (even in cold conditions), adequate rigidity, good thermal stability, and high resistance to chemical attack and environmental stress cracking” (p. 3658). Ghanbari, Salavanti-Niasari, Karimzadeh, and Gholamrezaei (2014) agree when stating that ABS is a highly sought-after thermoplastic in engineering due to its many desirable properties that include but are not limited to: “suitable mechanical properties, chemical resistance and appropriate processing characteristics” (p. 228).

Olivera et al. (2016) mentioned that many popular characteristics led to the use of ABS in areas such as molding, where parts such as pipes were produced. Eventually ABS found its way into areas of “textiles, fashion, toys, and domestic applications” in the 1950s. Within the 1990s, additive manufacturing technologies lead to the use of ABS within 3D-printing (p. 3658). According to Satches (2015), “The glass transition temperature of typical ABS is generally around 221 degrees Fahrenheit (105 degrees Celsius), and [the plastic] has an approximate melting or softening point between 401 and 473 degrees Fahrenheit (205 and 245 degrees Celsius), which allows for easy use in most commercial 3D-printers” (p. 8).

According to Savvakis, Petousis, Vairis, Vidakis, and Bikmeyev (2014), “ABS is a popular engineering thermoplastic, and it is the most common material used in fused deposition modeling (FDM) technology” (p. 1, Abstract). ABS can come in many chemical-make-ups such as but not limited to extrusion grade, plating grade, and molded grade (Matweb, 2017a); therefore, an appropriate chemical composition of ABS should be selected for a given application of extrusion. Some of the stipulations which can limit these abilities include but are not limited to: melt flow index, water absorption, tensile strength, and thermal conductivity

(Matweb, 2017b). Savvakis et al. (2014) gives insight into the popularity of research focused around this material when stating:

> Acrylonitrile-butadiene-styrene (ABS), because of these unique properties, such as an excellent mechanical response, chemical resistance, fine surface finish, and good processing characteristics, is widely used in various industries. For this reason several different studies determined the mechanical properties of this material and its composites under different conditions and to improve its mechanical properties (Savvakis, Petousis, Vairis, Vidakis, & Bikmeyev, 2014, p. 1).

These types of properties have potential to become enhanced through various methods. Vairis, Petousis, Vidakis, and Savvakis (2016) who examined the effect of strain rate on tensile strength of models build from ABS and ABS plus found that a thinner layer-thickness (as compared to all being tested) was the better choice for higher tensile strength results (p. 3563). These researched aimed to "determine how the mechanical strength of 3D printed parts is affected by different test speeds" (p. 3564). Tensile strength ranged between 3,190 psi (22 MPa) and 5,221 psi (36 MPa) for solid ABS 3D-printed samples with a ±45 degree infill angle (p. 3559-3560).

Tymrak, Kreiger, and Pearce (2014) found that it was "unclear as to whether the observed differences in mechanical properties were due to different layer heights and orientations or from other factors" (p. 5). These authors quantified "the basic tensile strength and elastic modulus of printed components using realistic environmental conditions for standard users of a selection of open source 3-D printers" (p. 1). The study "looked at the relationship between deposition patter orientation and layer height to tensile strength, strain at tensile strength, and modulus" (p. 2). They reported a final average tensile strength for their

3D-printed ABS parts to be 4,133 psi (28.5 MPa) (p. 6). The researchers brought up that many choices and other consideration need to be taken into account when producing parts on 3D-printers. Some of these include but are not limited to: “settings, tuning, and operation of each individual printer as well as the type, age, and quality of polymer filament used” (p. 6). The researchers conclude that “functionally strong parts can be created with open-source 3-D printers within the bounds of their mechanical properties” (p. 6).

Carbon Fiber Reinforcement (CFR) / Loading in 3D-Printing

Carbon fibers contain at least 92 wt% carbon (Huang, 2009, p. 2369) and are anisotropic (Kumata, Emori, Mitsumori, Watanabe, & Kobayashi., 1987). A fiber containing at least 99 wt% carbon is usually called graphite fiber (p. 2369). Having an anisotropic characteristic may add strength to 3D-printing materials in specific directions. Some of the physical characteristics which refer to the anisotropy of carbon fibers include but are not limited to: being brittle or easily damaged, does not absorb water, does not change their dimensions in humid environments (Vasiliev & Morozov, 2013, p. 12), and “yields different values of mechanical and thermal characteristics in the longitudinal and transverse directions” (Zoghi, 2014, p. 368). Tekinalp et al. (2014) researched “challenges and opportunities of fiber-reinforced composites made by 3D printing” (p. 145). These researchers “specifically evaluated the potential for load-bearing components...results show that composites with highly dispersed and highly oriented carbon fibers can be printed by FDM process [*sic*]” (p. 145). They found that fibers are mainly oriented in the direction in which the material is laid on the 3D-printer build-platform within specimen samples, therefore increasing tensile strength (p. 148).

Ning, Cong, Hu, and Wang (2017) and Tekinalp et al. (2014) collectively explain that carbon fibers have a high potential to support a load while the thermoplastic matrix binds, surrounds, and protects the carbon fibers and at the same time transfers the load to them. It should be noted that carbon fiber has a higher tensile strength than ABS (Fernandez-Vicente, Calle, Ferrandiz, & Conejero, 2016; Ma, Wang, Qi, & Jia, 2014) and therefore would logically work to support it when added into its chemistry. The general tensile strength displayed in related literature is about 725,000 psi (5 GPa) (Minus & Kumar, 2005; Seong-Mu et al., 2016). According to Shofner, Lozano, Rodriguez-Macias, and Barrera (as cited in Ning et al., 2015) "one of the possible methods is including reinforced materials (such as carbon fibers) into plastic materials to form thermoplastic matrix carbon fiber reinforced plastic (CFRP) composites" (p. 370). Biron (as cited in Ning et al., 2015) mentions that carbon fiber reinforcements in thermoplastics are being used in aerospace-engineering, automotive-industry, surgery/other medical procedures, and sustainability efforts (p. 370).

Review of tensile strength results using 3D-printable CFR ABS.

When deciding to use a filament loaded with reinforcement, an educated decision needs to be made in terms of how much of that reinforcement should be within the material before it becomes too much (i.e., reducing a needed strength or ability of a mechanical function). Tekinalp et al. (2014) assessed 0, 10, 20, 30, and 40 wt% carbon fiber loading within ABS at different fiber lengths; this procedure was then followed with tensile strength tests. Results indicated that 30 wt% yielded the maximum strength and 3D-printed reliably with tensile strength reported at about 8,702 psi (60 MPa). This amount was about 4,351 psi (30 MPa) more than with 0 wt%. At 40 wt%, the tensile strength was slightly higher (around 9,427

psi (65 MPa)); however, the 3D-printer's .02 inch (.5 mm) diameter nozzle would clog and create issues in the samples produced (p. 145 & 149). The issue of the clogging could have been due to many reasons such as but not limited to fiber loading, nozzle diameter, fiber length (designated as 3.2 mm (p. 145)), or fiber diameter.

Similarly Ning et al. (2015) experimented with 0, 3, 5, 7.5, 10, and 15 wt% carbon fiber reinforced ABS samples. Among other experimental results the results showed that 5% was the most effective in terms of tensile strength, reported as 6,091 psi (42 MPa), and reductions were seen between 5% and 10%; additionally, 7.5% performed better than 10% (p. 372). Through a microscopic investigation of the fracture surfaces of each broken specimen, Ning et al. (2015) concluded that the reductions were due to a non-uniform increase in porosity with the wt% of carbon fiber (p. 374). Additionally, their results showed that "many fibers had been pulled out of the matrix especially at 10 wt% carbon fiber content, indicating that the interfacial bonding between the thermoplastic matrix and carbon fibers was insufficient to provide satisfactory reinforcement in the composites" (p. 374-375).

Since some researchers report higher tensile strength results with 30% (Tekinalp et al., 2014, p. 145) carbon fiber loading and others report higher results at 5% (Ning et al., 2015, p. 376-377) suggests that there are variables along the methodological process of these research studies which could vary results. For instance, the length of carbon fibers might contribute to these different results. Ning et al. (2015) used chopped carbon fibers with a length of .15 mm (p. 372) while Tekinalp et al. (2014) used chopped lengths of 3.2 mm carbon fibers (p. 145). Other examples include: manufacturer of the materials used, 3D-printer type/quality, software settings, and ambient settings chosen for manufacturing of samples; each step may impact the

mechanical properties of resulting 3D-prints. Some settings which are beneficial to carbon fiber loading could have been used by one of the groups of researchers.

Satches (2015) took reinforcement levels from 5 wt% to 50 wt% graphene nanopowder within ABS and found that it is possible to load up to 50 wt%; however, only ABS with 10 wt% loading was 3D-printable. Five wt% ended up being the recommended level without modifications to a 3D-printer. The researcher utilized physical/visual analyses and statistical methods. Firstly, a Thermogravimetric analysis (TGA) was used to judge if "varying loading percentages was completed to determine if the addition of graphene was significantly changing the glass transition temperature of the material or if the material degradation temperature was experiencing any changes" (p. 12). Secondly, a Dynamic Mechanical Analysis (DMA) was completed to characterize "how the addition of graphene affects the viscoelastic properties of the printed part" (p. 28). The reported yield strength ended up being 5,293 psi (36.5 MPa) for 10 wt% and 5,579 psi (38.47 MPa) for 5 wt%. (p. 53). The researcher explains that poor dispersion of the graphene into the composite matrix is possible. After an investigation, two reasons were suggested as possible explanations for why an increase in carbon fiber loading led to a decrease in yield strength:

> First the bond between the ABS and the graphene at the molecular scale may not be as strong as predicted. Second it is difficult to verify that after extrusion and 3D-printing that agglomeration of the graphene is not occurring where the graphene may be restacking into graphite which is thereby creating stress concentrations in the material (Satches, 2015, p. 55).

Nakagawa, Mori, and Maeno (2017) worked with 3D-printing carbon fiber reinforced components by introducing fibers directly into the 3D-printer as it extruded plastic. These fibers are substantially longer than those used in other studies; however, this is meant to work towards an advantage of strength. Longer fibers could potentially mean more consistent strength across the specimen. These elongated strands of fibers were thermally bonded to the ABS through the use of a heating pin or a microwave oven to make thermal bonding-related comparisons (p. 2,815). Additionally, the "distribution of temperature of specimens just after heating" was given (p. 2815). The specimens which had a heating pin to weld the carbon fibers to the ABS had a tensile stress of about 5,511 psi (38 MPa), while the specimens thermally bonded using a microwave oven came in at about 5,438 psi (37.5 MPa) (p. 2816). At the beginning of the study, 10,732 psi (74 MPa) was mathematically predicted (p. 2814).

On the opposite end of the length spectrum, Li and Zhang (2009) reported on the uses of short-carbon-fiber (SCF)-reinforced thermoplastics (p. 537). These researchers report issues in terms of getting carbon fibers to adhere to ABS and they worked to enhance the adhesion between carbon fibers to ABS. Li and Zhang (2009) reported that "much research has been conducted to enhance the adhesion between carbon fibers and a polymer" (p. 537). To help with the bonding between carbon fibers and ABS, a surface treatment of HNO_3 was applied to the carbon fibers to break some of the double bonds between carbon atoms; however, this did not produce satisfactory results. They decided that another material would be involved with SFC-ABS called polyamide-6 (PA6) which has a terminal group that engages in acid/base interaction with the basic amino groups of the carbon, to help the carbon fibers adhere to the ABS and ultimately increase tensile strength (p. 541). Much like previous researchers

mentioned in this review, these researchers attempted many levels of the carbon fiber reinforcement to see which worked best. In this case, 0 wt% through 30 wt% in increments of 5 wt% were chosen - each containing its own ratio of PA6 (p. 538-539). The researchers used averaged results to graph and document the given results of tensile-tests, which included "the effects of SCF content on the tensile proper ties of ABS/SCF composites" (p. 539) and "the effect of incorporating PA6" (p. 541). Success was found with each of these levels, and tensile strength increased consistently (in a linear fashion) with each change in loading levels and surface treatments to the carbon fibers. These results follow what the researchers described as the Kelly and Tyson equation for short-fiber-reinforced composite materials. The researchers found "that, although the incorporation of HNO_3-treated SCFs improved the tensile properties, the desired bonding between carbon fibers and matrix was not achieved" (p. 541). At 30 wt% carbon fiber reinforcement, the tensile strength of the specimens were just above 13,053 psi (90 MPa). At 15 wt%, the tensile strength of these same specimens were about 10,152 psi (70 MPa). At 15 wt% SCF, PA6 was increased by ratio and the tensile strength also increased to about 14,793 psi (102 MPa) at a ratio of 3:7 (p. 539).

Manufacturers of 3D-printable CFR filament.

According to 3DX-Tech's (2017g) website, their CFR ABS "is made using 15 wt% high-Modulus Carbon Fiber (not carbon powder or milled carbon fiber)" (3DX-Tech, 2017g). This result means the formulation 3DX-Tech (2017g) came up with most-resembles the findings of Tekinalp et al. (2014); these researchers created their own material (p. 145). The company of 3DX-Tech (2017g) describes CarbonX™ CFR ABS as "a high-performance carbon fiber reinforced ABS filament ideal for anyone who desires a structural component with high modulus, excellent

surface quality, dimensional stability, light weight, and ease of printing" and is "made in the USA using premium Sabic MG94 ABS and high modulus carbon fiber". 3DX-Tech (2017g) offers other reinforced materials such as, but not limited to, nylon, polylactic-acid (PLA), and polycarbonate (PC) - each of which is offered with reinforcements with different additives such as, but not limited to, flame-retardants, glass-fibers, and electro-static displacers.

Other companies that offer reinforce 3D-printing materials (such as ABS) with additives (such as carbon fiber) includes, but is not limited to, the following:

- Oo-Kuma (2017) is a company based out of Delaware, USA and Istanbul, Turkey, which produces carbon fiber reinforced ABS, among other reinforced materials including, but not limited to, wood-reinforced PLA and other "high strength" and "medical grade" materials in which reinforcement properties are not.
- Airwolf3D (2017) is a company based out of California, USA, that sells reinforced 3D-printing materials including, but not limited to, carbon fiber reinforced ABS, PC, nylon, and polyethylene terephthalate glycol (PETG). This company also sells material reinforced to withstand high temperature and high-impact situations such as high-impact polystyrene.

Tensile Strength Differences based on 3D-Printed Infill Angle / Orientation

Three-D printed infill strands of plastic filament laid inside the area of shell strands (sometimes in a specified pattern or angle) as designated by software—can be created using different forms, such as solid or with geometric shapes. Solid components have many options in terms of how they are filled in such as angle to the longitudinal axis. When not using solid infills, shapes and patterns that work well for the model have been getting smarter as software has

improved. These shapes and custom infill options can be changed in size or density based on how much infill is needed. Baich (2016) advised that "typically, an infill density is selected as a percentage of cross-sectional area or categorical default settings, such as low and high density" (p. 12).

Baich (2016) investigated "infill designs, selection of printers, mechanical properties, and production costs" when referring to 3D-printing as a subject. The researcher explains that "among multiple process parameters that could impact the mechanical performance, infill design is often an overlooked aspect" (p. 11). The researcher sees a lack of information within software in terms of what is best for the model being printed. Mainly, this is because the commonly used software packages that create toolpaths for 3D-printer nozzles to follow as they build parts do not allow toolpaths to be changed, either to optimize 3D-printing efficiency or to optimize a particular mechanical property of the printed part, but instead allow users to select from a discrete number of choices for some parameters, such as infill pattern. This means mechanical properties of the component could be negatively influenced by the software's inability to adjust for material properties (p. 11-12).

This could also mean that the speed at which the nozzle is moving or how large the orifice on the nozzle is in comparison to that speed have an effect. Additionally, the orientation of the entire model - not just the infill - is an option to increase different strengths and change mechanical properties of models. Baich (2016) did not create any solid models; however, the researcher found that by comparing air gaps left by the infill shapes, tensile-testing results could be generated for mechanically inclined comparisons. By laying pairs of perpendicular layers, the most effective infill was found to be .04 inch (1 mm) air gaps laid at a 45[/-45]

degree infill orientation - or - the closest to a solid component made within the study which generated a tensile strength of 3,039 psi (20.96 MPa) (p. 49). The researcher concludes that "a wider variety of custom infill parameters should be printed and tested in order to note which infill has a higher impact on cost and strength" (p. 78).

Baich (2016) turned the entire model on the build-tray within the software before it was built as a way to shift the infill orientation. In other words, the infill angle to the x-axis of the build-tray was left the same in the software; simply changing the position of the model on the virtual build-platform in the software before it was built was enough to improve mechanical abilities (p. 26-27). Torrado et al. (2014) capitalized on this idea by 3D-printing solid components at two different orientations with the same infill orientation. These were designated as XYZ (on face) and ZXY (on end) - referring to their placement in relation to how the 3D-printer head lays strands. The "analysis was performed on the fracture surface of the tensile specimens through the use of scanning electronic microscopy" (p. 343, Abstract). Final results showed that too many cavities existed in the sample when the ZXY direction was used, and therefore it had a much lower tensile strength (p. 353). The XYZ direction resulted in a better tensile strength of 4,130 psi (28.5 MPa) while the ZXY direction resulted in 2,040 psi (14.1 MPa, p. 347).

As layers are stacked upon one-another during the FDM process, many opportunities exist for air-pockets and cavities which may take away from the model's tensile strength. Using a scanning electron microscope to examine the fracture surfaces of specimens 3D-printed at two different 3D orientations, Torrado et al. (2014) reported that the samples oriented in the ZXY orientation had many more cavities as well as lower tensile strength. These researchers

pointed out that the paths made for the infill "play an important role on the mechanical properties of the fabricated part due to the anisotropic nature of this fabrication technique" (p. 345). Their tensile strain results came to 4,133 psi (28.5 MPa) for their standard ABS and got up to 4,670 psi (32.2 MPa) with the additive titanium dioxide (TiO_2). These researchers found that, depending on the chemistry of their product, the amount in which the model was infilled changed slightly (p. 348). Within a model, more cavities in-between the strands also create an opportunity for mass to be affected as well as altering the mechanical strength of the 3D-printed part. While Torrado et al.'s (2014) specimens were within the ASTM standard, the difference in the material properties can have strength-altering effects on the 3D-printed model.

Similarly, Tymrak et al. (2014) concluded that 100% infill related prints still had "air gaps between extruded filament rasters that could not be specified...the actual positive or negative air gaps vary among printers due to printer differences" (p. 3). Final results of tensile-tests of their 3D-printed ABS components with pairs of perpendicular layers compared between their 0/90 degree and ±45 degree orientations. The latter of the two ended up being the strongest which came to a tensile strength of 4,133 psi (28.5 MPa) (p. 4-6).

Fernandez-Vicente et al. (2016) created tensile-testing specimens with different infill-patterns. This was specified as "the parameters evaluated in this study were the infill density and pattern. For the infill, three levels were evaluated: 20%, 50%, and 100%" (p. 186). The patterns chosen were "line, rectilinear, and honeycomb" (p. 186). Average tensile characteristics were recorded and compared. Additionally, a lack-of-fit test and an analysis of variance (ANOVA) test were completed. The researchers explained that "the statistical model

appears to be adequate for the observed data at the 95.0% confidence level" (p. 191). Since 100% infill was most effective in terms of tensile strength, significant differences were found between each of the patterns chosen for only the one infill density (p. 190-191). Conclusions were made that "the combination of rectilinear pattern in a 100% infill shows the highest tensile strength, with a value of 5,279 psi (36.4 MPa), a difference of less than 1% from that of raw (in this case, not 3D-printed) ABS material" (p. 191).

Hossain et al. (2013) studied improving mechanical properties of FDM-manufactured specimens many from polycarbonate using build-parameter modifications by using Insight software to change parameters, such as "build orientation, raster angle (RA), contour width (CW), numbers of contours, raster width (RW), raster to contour air gap, raster air gap (RRAG) and slice height" (p. 381). When the build-platform was being adjusted between angles and materials within their study, each of these parameters listed was being altered. The most important components for the study was the raster width (infill strand width) and contour width (shell strand width) which, together, designate if the strand being laid will touch and weld to the strand that has been previously laid beside-/-before it. Within Hossain et al.'s (2013) study, the model itself was not adjusted, but the infill orientation was changed instead. By laying pairs of perpendicular layers, three different RAs were used: 0/90, 30/-60, and 45/-45 degrees" (p. 383). In terms of tensile strength; the 45/-45 degree RA performed the best with polycarbonate (PC) at 7,795 psi (53.75 MPa), which was predicted by the researchers to be about double what ABS would have achieved, which is about 3,898 psi (26.88 MPa) (p. 382 & 390).

Thakur (2017) examined the effects of processing parameters and product design on the strength and accuracy of 3D-printed parts in an effort to develop guidelines based on optimal parameters (p. iv). One step was "developing the statistical model for tensile strength for different orientation and infill patterns" when speaking about a list of ways to improve the tensile strength of 3D-printed items (p. 20). In this case, the researcher adjusted the orientations of both the infill and the model in the software before 3D-printing. Additionally, Thakur (2017) claimed that "air gap and layer thickness are the most significant parameters that affect the porosity and mechanical properties of the ABS scaffold structures" and adjusted the 3D-printer settings accordingly (p. 14 & 28-29). Utilizing Simplify3D (Version 4.0.0, 2017), software for sending 3D model information and build parameters to a 3D printer, the infill angle/orientation levels chosen were 0, 45; +45, +45; and 45, 90 degrees. Model orientations include X-Y, Y-Z, and Z-X; each of these axis designations relates to the model's axes during drawing, rather than to the axes involved in FFF (p. 25). Infill types used include vertical-rectilinear infill, horizontal-rectilinear, vertical-wiggle infill, and horizontal-wiggle infill (p. 29-30). Each "raster angle (R.A.)" also received an array of "layer thicknesses (L.T.)", "print speeds (P.S.)", and "part bed temperatures (P.B.T.)" (p. 28). The best tensile strength ended up coming from the specimens printed in a 0 degree R.A., .0059 inch (150 μm) L.T., 2,500 mm per min P.S., and 115 degrees Celsius P.B.T. within vertical-rectilinear orientation model form at 4,364 psi (30.09 MPa) (pp. 29 & 34).

Summary

Three-D printing has become an industrial trend as noted by Berman (2007) and furthermore should be considered for further research and testing (p. 2). Savvakis et al. (2014) praised the nature and popularity of ABS within 3D-printing. Overall, this literature review shows that using ABS as a 3D-printing material is an effective way to assure that results are mechanically sound and applicable to current 3D-printing applications (p. 1, Abstract). Shofner, Lozano, Rodriguez-Macias, and Barrera (2003) conclude that utilizing reinforcements in 3D-printing materials is a practiced component of additive manufacturing (as cited in Ning et al., 2015, p. 370). Carbon fiber is a good choice as an additive for this study due to its naturally displayed tensile strength as reported by Ma, Wang, Qi, and Jia (2014); Minus and Kumar (2005); and Seong-Mu et al. (2016). However, adhesion between ABS and carbon fiber has not been ideal (Li and Zhang 2009, p. 537). Carbon fiber tensile strength differs greatly from that of ABS as shown by Tymrak et al. (2014, p. 4) which will help drive conclusions when comparing materials. Support is given by Torrado et al. (2014) that infill plays an important role in the tensile strength of fabricated items (p. 345). Baich (2016) and Hossain et al. (2013) collectively report that infill angle alterations cause differences in tensile strength results, therefore, supporting the current study's efforts.

Chapter 3: Methods

The methodology describes actions which were performed and documented including: research approach & design, material preparation and properties, 3D-printer preparation, manufacturing samples with specified infill orientations, tensile-testing samples as specified by an ASTM standard, and data analysis. The goal in methodology was to collect and analyze tensile strength data which then shows the effect of carbon fiber on ABS and infill angle on the 3D-printed parts when referring to tensile strength.

Research Design and Sample

A between-group experimental design was used to examine the main effects of two independent variables (type of material and infill angle) on the tensile strength of specimens conforming to the Type 1 specification of the ASTM standard D638: Standard Test Method for Tensile Properties of Plastic (Appendix-A). ASTM (2012) states that the number of specimens tested must be "7.2 Ten specimens, five normal to, and five parallel with, the principle axis of anisotropy, for each sample in the case of anisotropic materials" (p. 51). With six levels of infill angle, fifteen pair-wise comparisons were possible. Therefore, in light of the need to use a Bonferroni transformation, a total of fifteen test specimens were built per experimental group (180 specimens), with three extra specimens if an original specimen in the group had to be discarded (180+36=216 in total). Specimens were grown with their faces parallel to the build-platform with no supports, rafts, or brims. All specimens were manufactured with the Flashforge Creator Pro 3D-printer using ABS and CFR ABS filament from 3DX-Tech (2017a) at six infill angles. This resulted in 12 groups of 15 specimens each (Table 1).

Table 1.

Comparison Groups

	Type of Material	
Infill Angle (degrees)	ABS (count)	CFR ABS (count)
15	15	15
30	15	15
45	15	15
60	15	15
75	15	15
90	15	15

Material

While this study took place, only one supplier was available for the carbon fiber reinforced ABS. The ABS (designated "Natural ABS" by 3DX-Tech, 2017f) used is similar to the ABS used with the carbon fiber reinforcements; having ABS that is also a part of (or similar to) the ABS within the CFR ABS is desired for consistency and relatability in results. Natural ABS filament and 15 wt% carbon fiber reinforced ABS (both .07 inch (1.75 mm) ±.002 inch (.05 mm) diameter) were obtained from 3DX-Tech (2017f; 2017g). 3DX-Tech (2017f) describes the ABS (CAS No. 9003-56-9) as "made in the USA using 100% virgin resin and colorants - precision extruded onto 2.2 lb (1 kg) reels. The filament is then vacuum-sealed with desiccant to protect it from moisture" (3DX-Tech, 2017f). It should be noted that ABS is hygroscopic and therefore needs to be kept as dry as possible. 3DX-Tech's (2017f, 2017g) carbon fiber (CAS No. 308063-67-4) reinforced ABS (CAS No. 9003-56-9) "is made using 15 wt% High-Modulus Carbon Fiber (not carbon powder or milled carbon fiber). [*sic*] Made in the USA using premium Sabic MG-94 ABS" (2017g, page #). The specific tensile strength of the fibers being used in the carbon fiber reinforced ABS material within this study were not specified. The CFR ABS was wound into 1.1

lb (500g) reels in this particular study based on what was ordered. 3DX-Tech (2017f & 2017g) reported that both materials work with the Flashforge 3D-printer series.

3DX-Tech (2017a), the supplier of the ABS material provided no data regarding the chemistry, melt flow index or manufacturer of the ABS original resin. Technical information about the natural ABS can be found in Appendix-B. A Tinius Olsen^{TM} MP 987 extrusion plastometer was used to test the melt flow of the natural ABS (in accordance with ASTM D1238 (2013)); these values can be found in Table 2. More information about the ABS within the CFR ABS can be found in Appendix-F.

Table 2

Melt Flow Index (grams/10 minutes)

Natural ABS	ABS within CFR ABS	CFR ABS
2.5 g/10 min	11.7 g/10 min (Matweb, 2017c)	3.5 g/10 min

These melt flow index values are in the range for extrusion grade material, and therefore are likely to perform satisfactory during 3D-printing. The lower value for the CFR ABS could be a reason to consider using slower nozzle travel speeds. With speculation, melt flow index values could contribute to bonding related issues between carbon fiber and ABS.

According to 3DX-Tech (2017b), the tensile strength of the natural ABS obtained from them is 5,946 psi (41 MPa). Matweb (2017c) has chemistry and technical information about the Sabic ABS used within the Carbon Fiber Reinforced ABS composite such as melt flow index and density. The reported tensile strength of the Sabic ABS is 5,076 psi (35 MPa) (Matweb, 2017c). Technical information about the carbon fiber reinforced ABS can be found in Appendix-D. According to 3DX-Tech (2017d), the tensile strength of the reinforced ABS is 6381 psi (44 MPa).

The tensile strength of the carbon fiber used within the reinforced material was not listed by 3DX-Tech (2017d). Safety information about both materials can be found in Appendices C and E respectively.

In this study, most of a single 2.2 lb (1 kg) spool of ABS was required, and three 1.1 lb (500 g) spools of carbon fiber reinforced ABS were needed, but only part of the third spool was used. Once finished, and during times when the machine was not in use throughout the study, the spools of material were unloaded from the 3D-printer and stored in sealable Mylar bags with desiccant.

3D-Printing

3D-Printer software preparation.

The electronic file of the specimen created in a 3D-graphical environment (see Appendix-A) was imported into Simplify3D (Version 4.0.0, 2017) through a stereolithography (.STL) file. Build parameters included the following:

- nozzle temperature: 446 Fahrenheit (230 Celsius)
- build-platform temperature: 230 Fahrenheit (110 Celsius)
- extrusion speed: 141.73 in/min (3600.0 mm/min)
- infill percentage: 100
- number of perimeter shell layers: 2
- number of top and bottom shell layers: 0
- rafts, brims, supports: none
- layer height: .2 mm

The default setting which designates the first layer-height to be 90% of normal layer height was changed to 100%. This adjustment means 16 even layers at .008 inch (.2 mm) thick each stacked to produce a .126 inch (3.2 mm) thick sample. The default software settings for the 3D-printer can be found in Appendix-G.

Simplify3D (Version 4.0.0, 2017) software and a Flashforge Creator Pro 3D-printer were used to manufacture the samples. A .016 inch (0.4 mm) diameter nozzle was used. The build-platform was covered with a 0.25 inch (6.35 mm) tempered glass platform. This was lightly coated with a solution of ABS in acetone to improve first layer adhesion and was reapplied as needed. The build-platform was leveled with a .003 inch (.07 mm) thick leveling card supplied by Flashforgeusa (2017) prior to the first build for each experimental group, i.e., the initial distance of the build-platform to the nozzle was established, and the build-platform was set parallel to the X/Y axis of the nozzle movement. Initial nozzle height was determined by visual inspection of the first build layer to achieve roughly 90% surface coverage by ABS. Specimens were built face-down, one at a time, with their longitudinal axis parallel to the x axis of the printer. The 3D-printer's acrylic enclosure was used so the build chamber temperature would be higher than room temperature. The nozzle and build-platform were preheated prior to a build, with adequate time to account for even distribution of heating for the glass build-platform.

Most of the procedures and specifications of the *ASTM D 638-02: Standard Test Method for Tensile Properties of Plastics* were followed. The tensile-testable *bone* (referring to its shape) can be found in Appendix-A. According to ASTM (2012), "6.1.3 Reinforced Composites – The test specimen for reinforced composites … shall conform to the dimensions of the Type I

specimen…" (ASTM D 638 – 02, p. 50). Each specimen was measured to ensure it was within specifications for ASTM tensile-testing, then labeled and placed into an air-tight bag with desiccant. Build material was unloaded and returned to an air-tight bag with desiccant when not in use.

Figure 1 shows a print-preview of each infill angle with designated predetermined strand-path in which the software followed. Note that this preview only shows one layer; therefore, an assumption should be made that the next layer is opposite (e.g., -15 to +15) to the one seen in Figure 1 (with the exception of the 0/90 specimen).

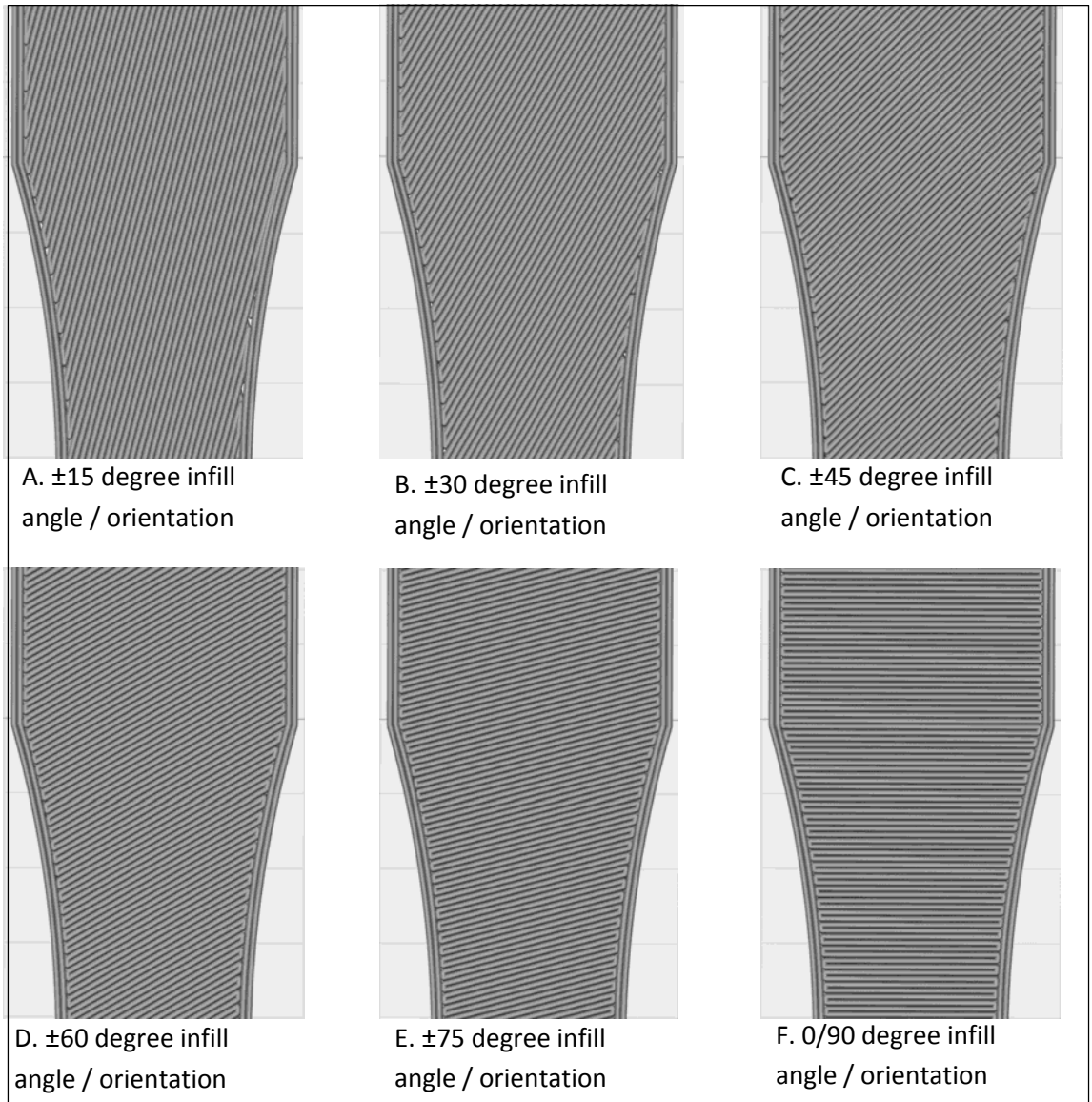

Figure 1. Print-preview within the software of a bone sample per each infill orientation.

Manufacturing tensile-test samples.

Once the machine was pre-heated, the software sent the file / associated nozzle paths to the machine. When each sample was completed, the specimen was removed from the machine, and a new layer of ABS/Acetone slurry was laid before the next 3D-print was started. As each of the eighteen specimens in the experimental group were built, they were labeled and

sealed in an air-tight bag with desiccant immediately after each 3D-print. Labels designated top/bottom of the specimens and physical order within the groups.

With both ABS and CFR ABS, when the next orientation was started, slight adjustments needed to be made to the wing-nuts underneath the build-platform to help create a solid and testable specimen (i.e., within the constraints of the ASTM standard). A leveling card that came with the 3D-printer was used to level the build-tray; however, without further adjustments to the height of the build-tray, some strands being laid would not stick to another strand previously laid completely per-infill-angle. This was overcome by performing a preliminary 3D-print of the first specimen within each group. When the first layer was extruded onto the build-surface, cohesion between the strands was visually inspected. If cohesion between the strands was not sufficient (see Figure 2), spaces would exist between each strand, and the platform would be adjusted closer to or further from the nozzle (allowing for more or less “squish” of the material to cohere). The strands not cohering properly created a problem with porosity of the specimen. Holes were created by insufficient strands being laid perpendicular to one another layer-by-layer. If holes exist within the specimen (as seen in Figure 3), the specimen being tested is not solid as specified by this study. If cohesion was sufficient where no visible spaces between strands (see Figure 4), a second layer was allowed to print. If scraping of the nozzle audibly occurred against the specimen as the second layer was extruded on top of the first, the platform would be slightly lowered (therefore allowing more space between the nozzle and the build-surface) and a second preliminary print would be done to assure strands were still cohering together sufficiently and no scraping was occurring on the proceeding layer.

Figure 2. Single-layer example of bad tensile-testing specimen due to insufficient cohesion between strands. 45 degree infill angle used.

Figure 3. Two-layer example of bad tensile-testing specimen due to insufficient cohesion between strands. ±45 degree infill angle used.

Figure 4. Single-layer example of good bone specimen due to sufficient cohesion between strands. 45 degree infill angle used.

Size measurements.

The width and thickness of each Type I bone sample was measured with "a suitable micrometer to the nearest .001 inch (.025 mm) at several points along the narrow section" (ASTM D 638 – 02, 2012, p. 52). These measurements can be found in Appendix-H. The ASTM (2012) standard does not specify which of the several points along the narrow section should

be entered into the software associated with the tensile-tester to specify dimensions of each specimen tested. Therefore, the smallest (marked with a yellow highlight in Appendix-H) measurement taken per width and thickness was used because this would be the point most expected to break during tensile-tests, since the least amount of material resides in that measurement location.

Tensile-Testing

A United Smart Test System SFM (22,480.9 lbf; 100 KN) equipped with a single piece of proprietary software, Datum, version 5 (United Testing Systems Incorporated, 2017), was used for testing all samples. The class B2-2 extensometer was included in order to determine modulus of elasticity; however, a secondary transverse strain measuring device was not included with the machine. This means that modulus of elasticity was calculated and Poisson's ratio was not.

United Testing Systems Incorporated 5 (2017) reported tensile strength at yield, tensile strength, tensile strain at yield, tensile strain at break, percent elongation, percent elongation at yield, percent elongation at break, and modulus of elasticity. As shown in Figures 5 and 6, graphs were generated for each specimen which depicts the strength-to-elongation curve.

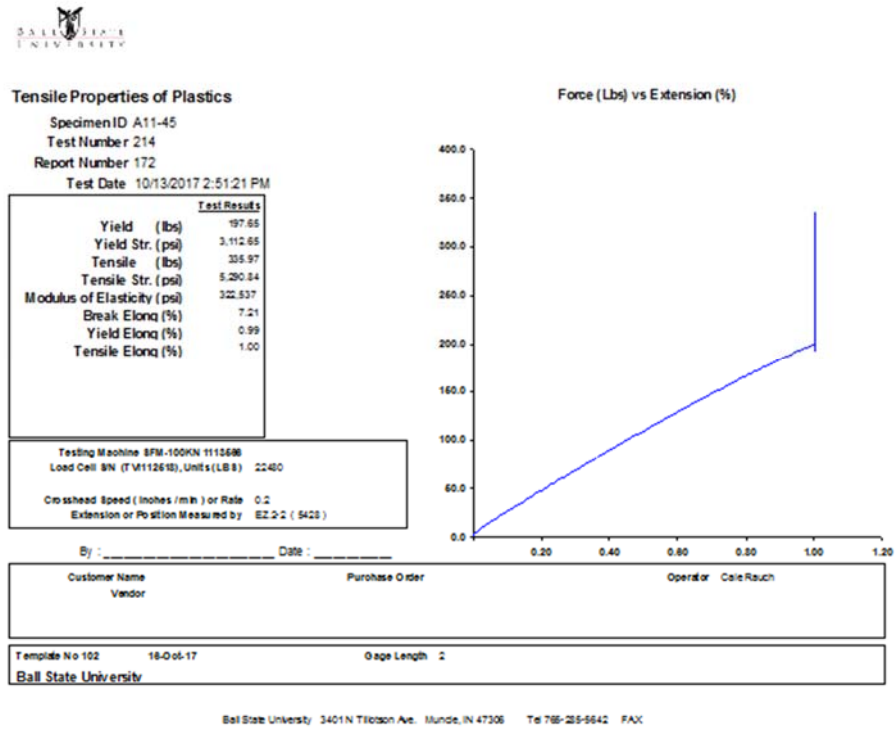

Figure 5. Example of report for ABS tensile-testing results supplied by Datum 5 (2017). Specimen A11-45 randomly chosen for display.

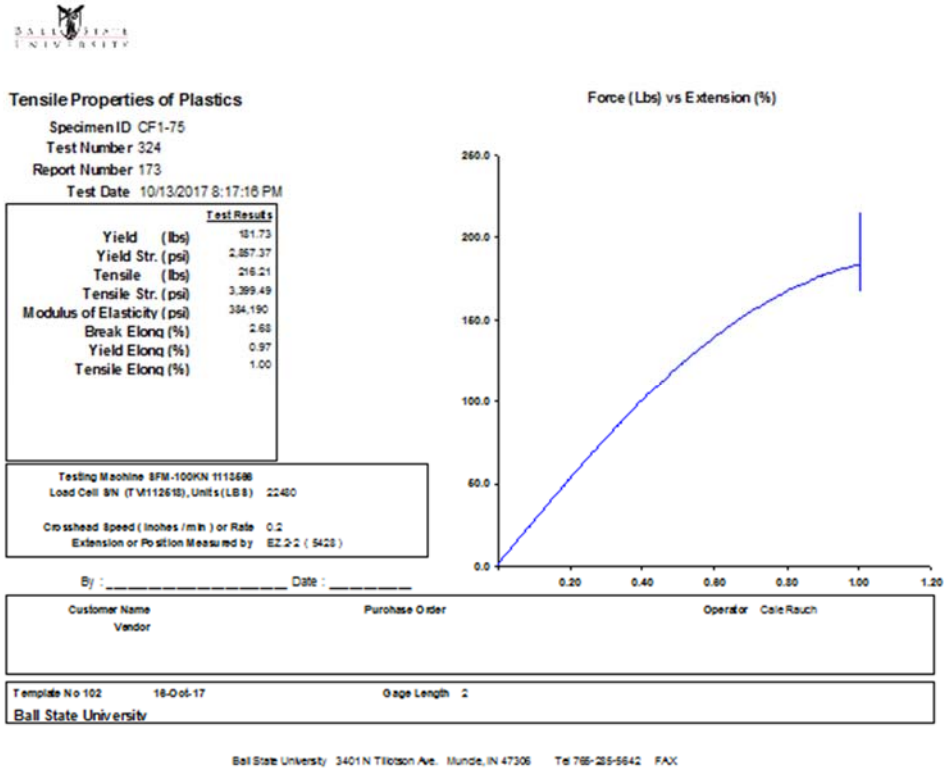

Figure 6. Example of report for CFR ABS tensile-testing results supplied by Datum 5 (2017c). Specimen CF1-75 randomly chosen for display.

Data Analysis

Data were analyzed using IBM SPSS Statistics version 25 (2017). One-way analyses of variance (ANOVA) and univariate analyses (extension of general linear model, GLM) with an alpha level of α=.01 were used to view between-subject effects of material and infill angle on the tensile strength data (See Appendix-H). *Tensile strength* was chosen as the measure to be analyzed because the *tensile strength at yield* results were suspected for inaccuracy and therefore could not be tested. Conclusions about significant differences between the mean strengths of samples by infill angle and material were analyzed.

Chapter 4: Results

This chapter will display each research question, information about the analysis completed for the research question, and display statistical tabled and graphed results. Discussions about these results are in Chapter 5.

Table 3 and Figure 7 show the results of tensile testing for infill orientation and material. Tensile strength averages ranged from 6,858 psi (±15 degree infill angle with ABS; 47.29 MPa) to 3,586 psi (±75 degree infill angle with CFR ABS; 24.73 MPa). The overall average strength was 5,338 psi (36.81 MPa) for ABS specimens and 4,786 psi (33.01 MPa) for CFR ABS, a mean difference of 551 psi (3.79 MPa).

Table 3 provides standard error and 99% confidence intervals of each mean tensile result per infill angle of each material. This interval shows that if an infinite amount of tests were completed; the proportion of those intervals which contain the true value of the parameters will match the confidence interval within the lower and upper bound displayed on the table. With the exception of the 0/90 degree infill, tensile strength generally increased as the infill angle orientation generally decreased.

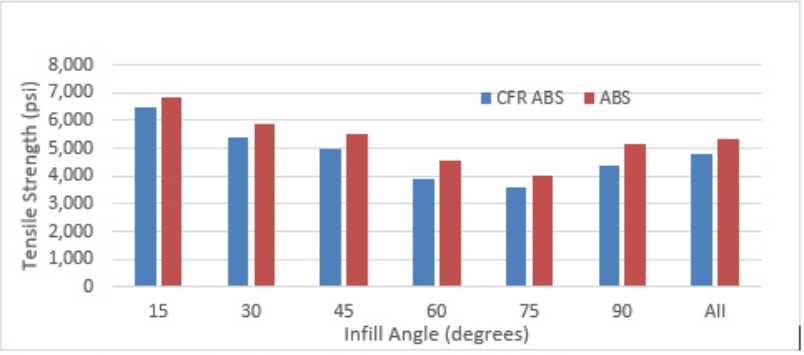

Figure 7. Average Tensile Strength by Material and Infill Angle

Table 3

Mean of Tensile Strength and Confidence Intervals by Independent Variable

Material	Angle (°)	Tensile Strength Mean (psi)	Std. Deviation	99% Confidence Interval Lower Bound	99% Confidence Interval Upper Bound
ABS	15	6858.835	40.90	6677.346	7040.323
	30	5877.935	71.33	5696.447	6059.424
	45	5531.907	520.95	5350.418	5713.395
	60	4552.722	283.83	4371.234	4734.210
	75	4022.707	105.66	3841.218	4204.195
	90	5186.633	238.47	5005.144	5368.121
CFR ABS	15	6492.481	239.53	6366.763	6618.198
	30	5420.633	147.65	5294.915	5546.350
	45	4961.540	229.35	4835.822	5087.258
	60	3906.374	161.94	3780.656	4032.092
	75	3586.929	199.60	3461.211	3712.646
	90	4353.919	83.27	4228.202	4479.637
Overall	15	6675.658	251.43	6566.534	6784.781
	30	5649.284	258.97	5540.161	5758.407
	45	5246.723	490.45	5137.600	5355.847
	60	4229.548	399.49	4120.425	4338.671
	75	3804.818	271.54	3695.694	3913.941
	90	4770.276	458.40	4661.153	4879.399

Per each research question, a one-way ANOVA or a univariate analysis with tests of between-subject effects was completed to find if significance (α =.01) exists between variables. When significance was found, a post hoc analysis was conducted. While the ANOVA can utilize a multiple comparisons post hoc with 99% confidence intervals, the univariate analysis does not have this function and a post hoc was not possible through SPSS (2017); therefore, pairwise multiple comparisons with 99% confidence intervals were performed. A critical level of significance has been adjusted by *p*=.01 and was divided by 15 (i.e., total number of pairwise

comparisons (m); $p = \alpha/m$, therefore $p = .01 / 15 = .000667$) using a Bonferroni correction to help control Type-I error through multiple comparisons.

How does infill angle affect the tensile strength of solid 3D-printed ABS samples?

In terms of tensile strength, infill angles were statistically different, $F(5)=211.39$; $p<.01$, for the ABS group (see Table 4). Pairwise comparisons (Table 5) showed significant differences between all infill angles. With the exception of the 0/90 degree infill, tensile strength increased as the infill angle orientation of the specimens decreased. The highest average tensile strength occurred at the 15 degree infill angle (6,858 psi; 47.29 MPa).

Table 4

ANOVA: Effect of Infill Angle on Tensile Strength of ABS

	Sum of Squares	df	Mean Square	F	Sig.
Between Groups	75174554.296	5	15034910.859	211.389	.000
Within Groups	5974453.561	84	71124.447		
Total	81149007.856	89			

Table 5

Multiple Comparisons between Infill Angle for ABS

(I) Infill Angle (°)	(J) Infill Angle (°)	Mean Difference (I-J) (psi)	Std. Dev.	Sig.	99% Confidence Interval	
					Lower Bound	Upper Bound
15	30	980.89933*	86.15	.000	636.6766	1325.1221
	45	1326.92800*	522.22	.000	982.7053	1671.1507
	60	2306.11267*	292.91	.000	1961.8899	2650.3354
	75	2836.12800*	123.34	.000	2491.9053	3180.3507
	90	1672.20200*	242.70	.000	1327.9793	2016.4247
30	45	346.02867*	528.71	.009	1.8059	690.2514
	60	1325.21333*	302.70	.000	980.9906	1669.4361
	75	1855.22867*	152.89	.000	1511.0059	2199.4514
	90	691.30267*	252.19	.000	347.0799	1035.5254
45	60	979.18467*	580.77	.000	634.9619	1323.4074
	75	1509.20000*	547.46	.000	1164.9773	1853.4227
	90	345.27400*	438.10	.010	1.0513	689.4967
60	75	530.01533*	248.18	.000	185.7926	874.2381
	90	-633.91067*	333.40	.000	-978.1334	-289.6879
75	90	-1163.92600*	222.40	.000	-1508.1487	-819.7033

Note. Bonferroni adjustment used.
*. The mean difference is significant at the .01 level.
Dependent Variable: Tensile Strength.

How does infill angle affect the tensile strength of solid 3D-printed CFR ABS samples?

For CFR ABS specimens, the ANOVA test revealed a significant difference in tensile strength by infill angle ($F(5, 84)=504.91$; $p<.01$) (see Table 6). The multiple comparisons in Table 7 show significant differences existed between all pairs of infill angles. With the exception of the 0/90 degree infill, tensile strength increased as the infill angle orientation of the specimens decreased.

Table 6

ANOVA: Effect of Infill Angle on Tensile Strength for CFR ABS

	Sum of Squares	df	Mean Square	F	Sig.
Between Groups	86157766.357	5	17231553.271	504.906	.000
Within Groups	2866771.779	84	34128.235		
Total	89024538.136	89			

Table 7

Multiple Comparisons between Infill Angles for CFR ABS

(I) Infill Angle (°)	(J) Infill Angle (°)	Mean Difference (I-J) (psi)	Std. Dev.	Sig.	99% Confidence Interval	
					Lower Bound	Upper Bound
15	30	1071.84800*	325.61	.000	833.4037	1310.2923
	45	1530.94067*	286.35	.000	1292.4963	1769.3850
	60	2586.10667*	289.95	.000	2347.6623	2824.5510
	75	2905.55200*	240.34	.000	2667.1077	3143.9963
	90	2138.56133*	258.18	.000	1900.1170	2377.0057
30	45	459.09267*	303.37	.000	220.6483	697.5370
	60	1514.25867*	180.61	.000	1275.8143	1752.7030
	75	1833.70400*	306.67	.000	1595.2597	2072.1483
	90	1066.71333*	186.17	.000	828.2690	1305.1577
45	60	1055.16600*	278.74	.000	816.7217	1293.6103
	75	1374.61133*	281.48	.000	1136.1670	1613.0557
	90	607.62067*	201.97	.000	369.1763	846.0650
60	75	319.44533*	223.64	.000	81.0010	557.8897
	90	-447.54533*	172.59	.000	-685.9897	-209.1010
75	90	-766.99067*	218.66	.000	-1005.4350	-528.5463

Note. Bonferroni adjustment used.
*. The mean difference is significant at the .01 level.
Dependent Variable: Tensile Strength.

What differences exist in tensile strength of ABS and CFR ABS at a given infill orientation?

A univariate analysis for between-subjects effects was completed to test the differences between ABS and CRF ABS in terms of the mean tensile strength of each infill angle.

This tested the null hypothesis that there is no difference between materials (ABS and CFR ABS) in terms of the mean tensile strength of a solid, 3D printed part at a single infill angle. There was a significant difference ($F(1, 28)=67.84$; $p<.01$) difference found (see Table 8). Pairwise comparisons were performed. The pairwise comparisons for means per infill angle by material shows that significant differences exist between all infill angles of each material (see Table 9). The pairwise comparisons for means per infill angle regardless of material also show that significant differences exist between all infill angles (see Table 10).

Table 8

Tests of Between-Subjects Effects of Material on Tensile Strength

Source	Type III Sum of Squares	df	Mean Square	F	Sig.
Intercept	4613600033.537	1	4613600033.537	22869.794	.000
Material	13685715.184	1	13685715.184	67.841	.000
Error	5648533.660	28	201733.345		

Table 9

Pairwise Comparisons for ABS and CFR ABS Tensile Strength Means by Infill Angle

Angle (°)	(I) Material	(J) Material	Mean Difference (psi) (I-J)	Std. Error	Sig.[a]	99% Confidence Interval for Difference[a]	
						Lower Bound	Upper Bound
15	ABS	CFR ABS	366.354*	62.740	.000	192.986	539.722
30	ABS	CFR ABS	457.303*	42.338	.000	340.312	574.293
45	ABS	CFR ABS	570.367*	146.968	.001	164.256	976.477
60	ABS	CFR ABS	646.348*	84.374	.000	413.201	879.495
75	ABS	CFR ABS	435.778*	58.312	.000	274.646	596.910
90	ABS	CFR ABS	832.713*	65.219	.000	652.497	1012.930

*. The mean difference is significant at the .01 level.

a. Adjustment for multiple comparisons: Bonferroni.

Table 10

Pairwise Comparisons for Tensile Strength Means Regardless of Material

(I) Infill Angle (°)	(J) Infill Angle (°)	Mean Difference (I-J) (psi)	Std. Dev.	Sig.[a]	99% Confidence Interval for Difference[a]	
					Lower Bound	Upper Bound
15	30	1026.374*	235.55	.000	859.958	1192.789
	45	1428.934*	426.62	.000	1134.669	1723.2
	60	2446.110*	319.81	.000	2242.473	2649.746
	75	2870.840*	190.99	.000	2737.369	3004.311
	90	1905.382*	341.85	.000	1730.307	2080.456
30	45	402.561*	427.41	.000	101.388	703.733
	60	1419.736*	263.10	.000	1245.579	1593.893
	75	1844.466*	238.34	.000	1675.158	2013.774
	90	879.008*	289.63	.000	724.13	1033.886
45	60	1017.175*	449.26	.000	698.891	1335.459
	75	1441.906*	433.15	.000	1137.757	1746.054
	90	476.447*	360.76	.000	238.094	714.8
60	75	424.730*	255.63	.000	259.671	589.79
	90	-540.728*	277.53	.000	-726.219	-355.237
75	90	-965.458*	296.15	.000	-1119.56	-811.361

Note. Based on estimated marginal means

*. The mean difference is significant at the .01 level.

a. Adjustment for multiple comparisons: Bonferroni.

Tables 11 and 12 demonstrate the differences between the materials in terms of tensile strength when referring to the means of all specimens at all infill angles in one numerical data point. The pairwise comparisons (Table 12) generated for these combined means show that a significant difference exists between the two materials overall when referring to all infill angles as one mean. Throughout each comparison, tensile strength averages of ABS were significantly greater than tensile strength of CFR ABS per each infill angle. Together, all pairwise

comparisons (Tables 9 through 12) demonstrate that the tensile strength measures of ABS were, on average, higher than the measures of CFR ABS per each infill angle.

Table 11

Estimates of Pairwise Comparisons for ABS and CFR ABS

Material	Mean	Std. Error	99% Confidence Interval	
			Lower Bound	Upper Bound
ABS	5338.456	24.181	5275.454	5401.459
CFR ABS	4786.979	24.181	4723.977	4849.982

Table 12

Pairwise Comparisons for Means of All Infill Angles by Each Material

(I) Material	(J) Material	Mean Difference (I-J) (psi)	Std. Error	Sig.[a]	99% Confidence Interval for Difference[a]	
					Lower Bound	Upper Bound
ABS	CFR ABS	551.477*	34.198	.000	462.378	640.576

Note. Based on estimated marginal means

*. The mean difference is significant at the .01 level.

a. Adjustment for multiple comparisons: Bonferroni.

Post-Hoc Analysis of Filament

Table 3 and Figure 7 displays tensile strength averages per by material and infill angle with the same percentage comparison conducted. Overall averages indicate that CFR ABS was 90% as strong as ABS. This contradicts anticipated results that would suggest the adding of a reinforcement fiber would increase tensile strength rather than decrease it. Therefore, a post-hoc filament tensile test was performed in order to compare the tensile strength difference between CFR ABS and ABS filament that was used to 3D print specimens (see Table 13). Five strands of each type of 3D printer filament were tensile-tested. The results indicated that the CFR ABS filament was also 90% as strong as ABS filament; this conclusion fits the results seen in

Table 3 and helps to validate tensile testing results in terms of material difference across the current study.

Table 13

Post Hoc Filament Test Results by Material

Sample	Material	Dia (mm)	Force (MPa)	Strength (psi)	Mean (psi)	% Strength of ABS
1	ABS	0.068	23.4	6443.297		
2	ABS	0.068	24.0	6608.510		
3	ABS	0.068	23.7	6525.903		
4	ABS	0.068	23.4	6443.297		
5	ABS	0.068	23.7	6525.903		
					6509.382	
6	CFR ABS	0.07	24.0	6236.275		
7	CFR ABS	0.07	19.6	5092.958		
8	CFR ABS	0.07	22.8	5924.462		
9	CFR ABS	0.07	23.4	6080.368		
10	CFR ABS	0.07	23.4	6080.368		
					5882.886	90.3755

Post Hoc Analyses of Mass

Post hoc analyses were also conducted to eliminate the influence of mass. The mass (in grams) of each sample was recorded. In Figures 8 and 9 the results of tensile strength for natural ABS and CFR ABS samples respectively can be seen on a plot, to help visually demonstrate how the tensile strengths correlated with the mass of each sample.

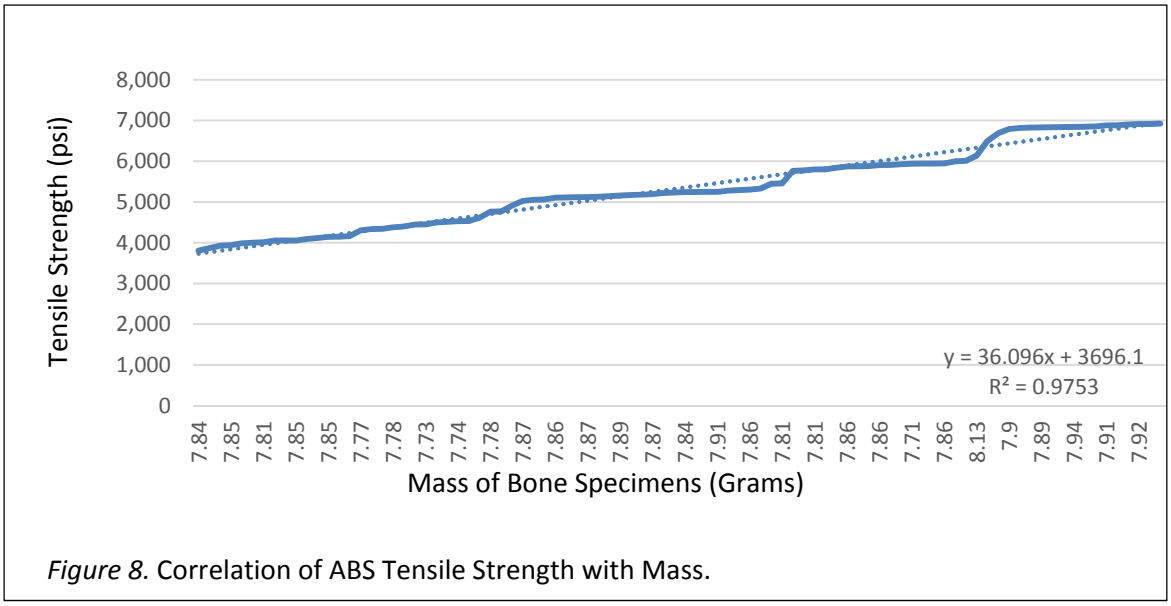

Figure 8. Correlation of ABS Tensile Strength with Mass.

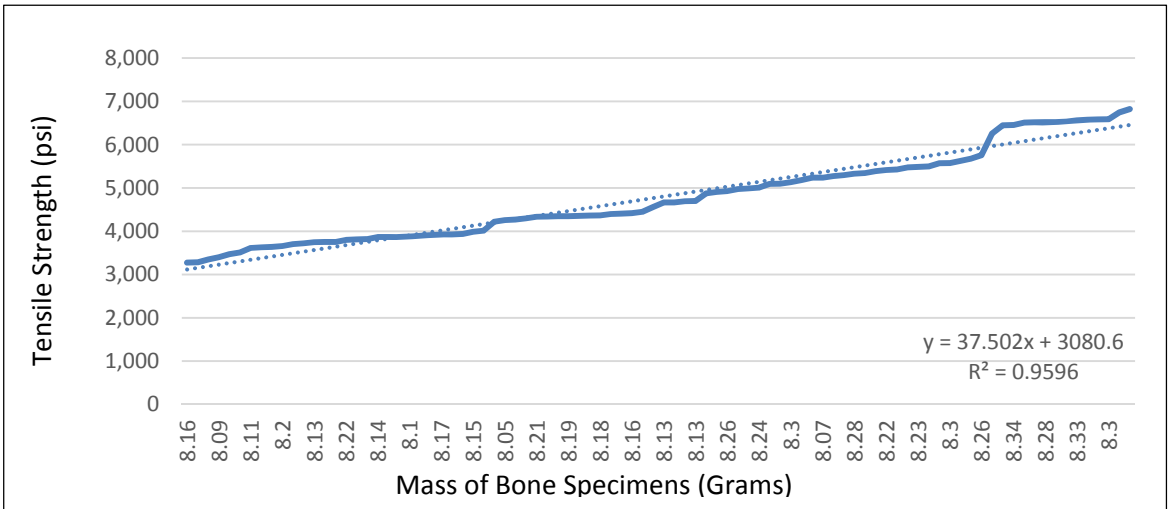

Figure 9. Correlation of CFR ABS Tensile Strength with Mass.

With an R^2-value of .97 for ABS and .95 for CFR ABS, mass could potentially be a time-varying (or time-dependent; i.e., seen as not constant through the entire study) covariate (i.e., a measurement that is not of primary interest but acting as a confounding variable). To test if this was the case, a univariate analysis was conducted to test between-subject effects of infill angle in terms of tensile strength while controlling for mass (Tables 14 & 15). The mass used for ABS and CFR ABS was the mean of each material's samples regardless of infill angle. Covariates were set to 7.87 grams for ABS and 8.21 grams for CFR ABS. Estimated marginal means adjusted by the covariate mass of ABS and CFR ABS samples can be found in Tables 16 & 17 respectively. Statistically significant differences were found in tensile strength ($F(5, 83)=159$, $p<.01$) between the infill angles of ABS while controlling for mass . Similarly for CFR ABS, statistically significant differences were found between in the tensile strength of infill angles ($F(5, 83))=295$; $p<.01$). Tables 14 & 15 have R^2 adjusted by the covariate mass. Generally, more massive samples had greater tensile strength.

Table 14
Tests of Between-Subjects Effects for ABS and Mass

Source	Type III Sum of Squares	df	Mean Square	F	Sig.
Corrected Model	75206801.537[b]	6	12534466.923	175.080	.000
Intercept	25463.982	1	25463.982	.356	.553
Mass	32247.242	1	32247.242	.450	.504
Infill Angle	57055475.780	5	11411095.156	159.389	.000
Error	5942206.319	83	71592.847		
Total	2646069449.918	90			
Corrected Total	81149007.856	89			

Note. R^2 = .927 (Adjusted R^2 = .921)

Table 15

Tests of Between-Subjects Effects for CFR ABS and Mass

Source	Type III Sum of Squares	df	Mean Square	F	Sig.
Corrected Model	86232662.311	6	14372110.385	427.270	.000
Intercept	7222.282	1	7222.282	.215	.644
Mass	74895.954	1	74895.954	2.227	.139
Infill Angle	49635180.724	5	9927036.145	295.122	.000
Error	2791875.825	83	33637.058		
Total	2151389844.795	90			
Corrected Total	89024538.136	89			

Note. R^2 = .969 (Adjusted R^2 = .966)

Table 16

Estimated Marginal Means for Tensile Strength of ABS Parts

			99% Confidence Interval	
Infill Angle (°)	Mean (psi)	Std. Error	Lower Bound	Upper Bound
15	6839.025[b]	75.127	6640.961	7037.088
30	5883.048[b]	69.505	5699.808	6066.287
45	5499.875[b]	83.969	5278.502	5721.248
60	4582.757[b]	82.314	4365.747	4799.767
75	4034.050[b]	71.123	3846.543	4221.556
90	5191.985[b]	69.545	5008.639	5375.330

b. Covariate: Mass = 7.8636 g.

Table 17

Estimated Marginal Means for Tensile Strength of CFR ABS Parts

Infill Angle			99% Confidence Interval	
(°)	Mean (psi)	Std. Error	Lower Bound	Upper Bound
15	6442.565[b]	57.978	6289.712	6595.417
30	5400.993[b]	49.150	5271.416	5530.570
45	4976.035[b]	48.341	4848.591	5103.479
60	3938.382[b]	51.986	3801.326	4075.437
75	3604.689[b]	48.828	3475.961	3733.416
90	4359.213[b]	47.487	4234.018	4484.407

b. Covariate: Mass = 8.2039 g.

Chapter 5: Conclusions & Recommendations

The purpose of this study was to determine the effect of infill angle (15, 30, 45, 60, 75, and 90 degrees) and material (ABS and CFR ABS) on the tensile strength of solid specimens made by 3D-printing. Utilizing the ASTM D638-02 (2012), 3D-printed tensile-testable specimens were grown. A between-group experimental design along with a statistical analysis were utilized to examine the main effects. The data-analysis showed that significant differences existed between each group of materials and the associated six infill angles / orientations. Tensile strength of ABS was consistently higher than CFR ABS with an average mean difference of 551 psi. Infill angles of ±15 degrees were the strongest and the infill angle of ±75 degrees was the weakest. Post hoc analyses controlling for mass also confirmed significant differences of infill angles for both materials.

Assumptions

It was assumed that the material obtained was consistent and the manufacturer's information was accurate. The melt flow index and general chemistry of each material was assumed to be consistent throughout the entire filament. The carbon fiber reinforced ABS was assumed to have consistent carbon fiber levels throughout the entire filament.

Limitations & Threats to the Validity

This section identifies potential weaknesses of the current study. Indoor temperature and relative humidity were not able to be controlled or measured and were assumed to be constant throughout the study.

Material.

The general chemistry, melt flow index and filament diameter of the ABS and CFR ABS tested in this study could be different than any other ABS or reinforced ABS on the market. Thus, these results may not be comparable.

3D-Printer and associated software.

When a 3D-printer is being calibrated, the platform-leveling is part of that process with the use of wing-nuts underneath the build-platform of the Flashforge Creator Pro. The point of the platform-leveling is to achieve two primary functions: create a *level surface* (seen here as where the build-platform surface is parallel with the x-y motion of the 3D-printer gantry) on which the nozzle extrudes the plastic for the nozzle to lay strands on, and for the nozzle to have enough room (where the gap between the nozzle and the surface at the initialization point are sufficient) to lay strands of material that "squish" around the circumference of the moving nozzle and melt and cohere into the strand previously left beside it. When making a solid model, all strands within each layer must cohere to the side of another strand and the previous layer or build-platform (if on the first layer) underneath. This makes leveling the entire build-platform (instead of just a section of the build-platform) much more difficult and sometimes impossible. This also makes printing more than one tensile-testing specimen difficult on this particular machine if identical and consistent models are wanted. Therefore, one tensile-testing sample was built at a time in the exact same place on the build-surface throughout the current study. With this being said, the build-platform leveling is a threat to the validity. During model production, each degree change (such as from ±45 degrees to ±60 degrees) within the infill orientation caused the need for a slight build-platform-leveling adjustment. There was no

pattern between where the build-platform needed to be and the specific infill-orientation that was being printed at the time. The same issue arose when switching between ABS and CFR ABS within the 3D-printer. So, while the strands still always "squished" together after a build-platform-leveling adjustment per-each-degree change, the strands and entire layers of material could have been touching/packing together slightly more or less each time, which could have caused unwanted changes in size variations across the specimen in the X/Y direction and changes in how tightly packed/cohered the layers became (i.e., the Z direction) - each of which could have changed the tensile strength. The fault in the final dimensions of the specimens showed up in post-measurements; however, none of the specimens were beyond ASTM specifications/tolerances (see Appendix-A). Even though all samples meet specifications, it is possible that one experimental group (i.e., one level of infill angle) has greater strength due to bonding between strands or entire layers due to changes in the platform leveling rather than due to infill angle.

Testing Equipment

The tensile-tester (United Smart Test System SFM (100 kN)) used was assumed to be sufficiently robust to still provide accurate and consistent readings even though its calibration (last calibrated on November 11, 2013) was expired (United Calibration Corporation, 2013). The tensile strength at yield listed in Appendix-H was suspected for inaccuracy. One interpretation of this data is that the tensile-tester was inaccurate and inconsistent. Another could be that the elastometer attached to each specimen was not working accurately. Calibration issues may have changed the ability for the software and the machine to communicate tensile strength at yield properly.

How does infill angle affect the tensile strength of solid 3D-printed ABS samples?

One purpose of this study was to determine how the tensile strength of solid 3D-printed ABS samples changes if their infill angle/orientation is altered. The data analysis showed that significant differences exist in between each group of the associated six infill angles / orientations. The tensile strength of natural ABS provided by 3DX-Tech (2017a) significantly changes based on the infill angle of the strands laid during the 3D-print. For the tests performed within this study, ±15 degrees had the greatest strength (when comparing any two infill angles) in terms of tensile strength. Other than 0/90 degree infill angle, tensile strength increases as the infill angle decreases. A conclusion can be made that a threshold in angular degrees exists in between ±15 and 0/90 degree infill orientation in which optimum tensile strength would exist.

A potential reason for the less significant differences may not have been as severe in the analysis between the ±45 and 0/90 degree infill angles could be due to components of the vector within each infill orientation being identical; however, while they are the same in terms vector and create the same right angle, the ±45 degree angle is turned (on its origin) in relevance to the longitudinal axis of the sample where the load is being applied. Changing where the force is being applied on the strands may not be affecting the overall specimen because the angle between each layer is still perpendicular - or - 90 degrees from the previous layer. As a counter example, when the ±15 degree infill strands are being laid, -15 degrees is not perpendicular to +15 degrees; together (one layer on top of another) the strands form an acute angle opening towards where the load is being applied and therefore creating a much

longer vector (in terms of magnitude directed where the force is being applied) than both ±45 and 0/90 degree infill angles.

How does infill angle affect the tensile strength of solid 3D-printed CFR ABS samples?

The infill angle was significantly different in terms of tensile strength for CFR ABS provided by 3DX-Tech (2017a). An infill of ±15 degrees had the highest tensile strength (Mean=6,492 psi; 44.76 MPa) and ±75 degrees had lowest (Mean= 3,586 psi; 24.73 MPa). This was likely due to the fact that the strands being laid were positioned closest to the length of the specimen without reaching 0/90 degrees. A conclusion can be made that a threshold exists in angular degrees between ±15 and 0/90 degree infill orientation in which optimum tensile strength would exist.

According to Tekinalp et al.'s (2014) study, carbon fibers tend to orient in the direction of the 3D-printed strands (p. 149). Therefore, it can be inferred that the vector analysis performed in the previous section applies to most of the fibers laid within the strands of ABS within each specimen. At a 0/90 degree infill orientation, some carbon fibers align parallel with the longitudinal axis (load bearing direction) of the specimen; however, half of those fibers (technically) are perpendicular to the loadbearing direction where they are not able to distribute as much of the load down the length of the fiber utilizing their anisotropic nature. But the perpendicular fibers are still taking up space within the ABS (where more ABS could otherwise reside) and therefore the specimen is withstanding less load overall. At a ±45 degree infill orientation, all the carbon fibers being laid on the build-platform are at least partially oriented in the load-bearing direction which could cause for a more significant difference

between the tensile strength of the two angles. More about material differences are discussed in the next section.

The results found for the effects of infill angle can be predicted by vector analysis, taking the square of the cosine of an angle to arrive at the percentage of total vector magnitude parallel to the longitudinal axis. As indicated in Table 18, this factor is 93% for the ±15° samples, decreasing to 75% for the ±60° samples. The ±45° and the 0/90° samples each had 50% of their vector magnitude parallel to the longitudinal axis. The factor falls to 25% and 7% for the ±30° and ±75° samples. It should be noted that the existence of shell strands and the zig-zag nature of infill strands decrease the predictive power based on vector analysis.

Table 18

Percentage of vector magnitude parallel to longitudinal axis.

Infill Angle (°)	$\cos^2$	Percentage
0	1	100%
15	0.933013	93%
30	0.75	75%
45	0.5	50%
60	0.25	25%
75	0.066987	7%
90	3.75E-33	0%

Notes. The average percentage for 0/90 is 50%.

What differences exist in tensile strength of ABS and CFR ABS at a given infill orientation?

The data-analyses show that significant differences exist in between each of the materials and within each group of the associated six infill angles / orientations (see Tables 10 through 14). ABS 3D-printed samples had significantly higher tensile strength than CFR ABS 3D-printed samples of the same infill angle (See Tables 3-5). By looking at the standard error on

Table 11, it can be seen that infill angle ±45 degrees had the greatest difference in tensile strengths between the two materials; otherwise, standard error for other infill orientations were close in value. The angle which had the least difference of tensile strength between the two materials was ±30 degrees. Keeping in mind that ABS is dominate over CFR ABS at every infill angle being studied when dealing with tensile strength, it should be noted that when comparing infill angles between materials, increases in the tensile strengths did not increase linearly with each infill angle.

A factor which could explain the greater strength of ABS over CFR ABS is how well the carbon fibers are adhering to the ABS. Li and Zhang (2009) tested a chemical surface treatment on the fibers after discussing that troubles existed when trying to adhere a carbon additive to a polymer, and that ample research has been completed on the subject when referring to other polymers (p. 537); therefore, similar issues could have existed in the current study and have been exacerbated (i.e., causing a lower tensile strength) when half of the fibers were oriented perpendicular to the load bearing direction. The difference of mean results (between ±45 and 0/90 degrees) given in Table 11 give traction to the idea that the carbon fibers may have given the ±45 infill oriented strands a better chance in the reinforced specimens based on their direction; however, ABS with no reinforcement still had larger tensile strength results for both ±45 and 0/90 degree infill orientations (see Tables 3 through 5); additionally, Table 13 and 14 each show that the average values of all angles per each material show dominance for ABS in terms of tensile strength. These results indicate that ABS would be a better choice as compared to CFR ABS for 3D model construction when maximizing tensile strength is a design goal.

It should be noted that while there is a strengthening of the specimen as the infill angle decreased and a weakening of the specimen as the infill angle increased, if the specimen had been pulled apart in its transverse direction (perpendicular to its axis) instead of its longitudinal direction, an opposite tensile effect of the infill strands would be predicted. In other words, increasing strength in one axis means a decrease in strength in the perpendicular axis, and it might be that this decreased strength is an issue for some manufactured parts.

Significance

Manufacturers and consumers could use the results of this study to potentially inform purchase decisions especially when higher tensile strength is desired in their 3D-printed models. This idea is not typical, as many 3D-printed parts are meant as rapidly produced prototypes, and not necessarily meant for bearing a load or being put under any kind of physical stresses. Additionally, many industries that represent areas of additive manufacturing, such as aerospace engineering and the medical field could benefit from understanding how reinforced composites compare to non-loaded materials when working with infill angle during the process of 3D-printing and finding a resulting tensile strength (or load capacity in general) of the model. This idea is especially relevant when referring to components being manufactured for technological advancements in the industry, which include 3D-printing working (sometimes load-bearing) parts instead of prototypes.

This study suggests that those at home with a 3D-printer could now be better informed about what angle to lay infill based on needs around the home or in personal work spaces. The findings could provide information useful in designing 3D-printed parts which are to be placed under stress.

Recommendations and Future Research

The results of this study indicate that the ABS used here is stronger than the CRF ABS used here at each infill level. These results contradict the proposition that adding carbon fiber reinforcement increases tensile strength (Ning et al., 2015, p. 372, 376-377). According to 3DX-Tech (2017b, 2017d), the tensile strength found from their tests with the natural ABS was 5,946 psi (41 MPa) (See Appendix-B), and identical tests with the carbon fiber reinforced ABS was 6,381 psi (44 MPa) (See Appendix-D); however, these results refer to the tensile strength at yield and not tensile strength when referencing to the current study. .

Carbon fiber reinforced material is noted as superior by companies who create, sell, and utilize this reinforced material for its designed purpose, which contradicts components of the current research when referring to tensile strength. More research is recommended in areas which compare the effect of infill angle on yield strength. This type of research may show that specific infill orientations should be specified when particular mechanical needs are required by the design of the model. .

It is recommended that future research examine more complex models which require different angle infill orientations to be grown. Umetani and Schmidt (2013) mention that "objects manufactured via layer-by-layer 3D-printing techniques such as FDM exhibit significant anisotropy; they can bear considerable tensile force in the direction of filament strands, while being rather fragile when forces perpendicular to the filament strands are applied" (p. 1). They present a "framework for structural weakness detection of 3D objects" in order to solve structural issues associated with infill angles / orientations of complex models in 3D-printing before sending the model and its settings from the software to the machine (p. 4). More

research should be completed which can specify what infill angles to use based on the material, model's requirements (i.e., types of strengths), and type of mechanical behavior needed by the model (i.e., model's functions).

The individual layer thickness that made up the tensile-testing specimens was set at .008 inch (.2 mm); however, in order to adjust for unforeseen changes in the printability of each infill angle, the initial build-platform height had to be adjusted per each infill angle / orientation, which effectively changed the layer thickness slightly. These changes had to be made to keep pores (air-gaps) from showing up in the finished model but could have caused problems with adhesion between the layers. More research is recommended to examine why the build-platform needed adjustment per each infill angle to avoid air gaps. These air gaps caused by layer-thickness issues are considered by Thakur (2017) to be the most important components which affect "mechanical properties" of ABS (p. 14).

More research should be done into how layer thickness affects tensile strength of models. This could be done by looking at the effect of the adhesion between the layers, which could not be effectively studied in the current study due to the slight adjustments of the build-platform between each infill angle / orientation during the 3D-printing process. More studies should be conducted which look at layer adhesion and if more (thinner) layers packed into the same model effectively create more adhesion and therefore more tensile strength. Had a different layer thickness been chosen, there is a chance that different results could have been seen across the current study in terms of tensile strength.

Carbon fiber is one of many additives that can be mixed with a common 3D-printing material like ABS to form a new composite material that is meant to overcome limitations that

the original 3D -printing material alone could not overcome. It was not known if any chemical treatments were given by 3DX-Tech (2017a) or by their supplier to the carbon fibers before being mixed with the ABS used in the current study to help with molecular adhesion. Researchers should examine the effect of additives to help with adhesion between the constituents of composite materials intended for 3D-printing (Li & Zhang, 2013).

3DX-Tech did not report the fiber lengths of the carbon in their CFR ABS. More research should be done on the effect of fiber length on the properties of 3D-printed specimens based on the results of Tekinalp et al. (2014) and Ning et al. (2015).

Aside from additives, other (non-reinforced) materials in general can be used to overcome limitations which reinforced materials could not overcome. Hossain et al. (2013) tried a different material (PC) as a choice to test 3D-printing properties; however, many other choices were available to the researchers such as "a PC-ABS blend, polyphenylsulfone (PPSF), ULTEM, and several varieties of the aforementioned materials designed for biocompatible or static dissipation applications" (p. 382). PC was meant to be so effective that ABS was not tested in that particular study, which help supports the recommendation for more research into the tensile strengths of other materials based on their infill orientations. Other materials which are stronger or more effective than natural ABS and CFR ABS could have different or otherwise more robust tensile responses to changed infill angles and become a more effective choice as a material-of-choice for tensile-bearing 3D-printed items.

For both the 3D-printed parts and the filament in which the parts were printed from, CFR ABS is about 90% as strong as ABS when utilizing 3DX-Tech's (2017f, 2017g) natural and carbon fiber reinforced ABS material and tensile strength. While manufacturing solid 3D-

printed models that are expected to withstand optimal tensile force until fracture, the choice for infill orientation is recommended to be ±15 degrees with both materials when being compared to the other infill angles in the current study and when referring to this particular manufacturer's materials; however, natural ABS was more effective. Further research is recommended in terms of how close-to-parallel with the longitudinal axis (in which the load is being applied) can be approached before tensile results start to decline and the range of infill angles / orientations between ±15 degrees and 0/90 degrees infill orientations (such as ±10 degrees).

References

3DX-Tech. (2017a). *Technology… advanced*. Byron Center, MI. Retrieved from http://www.3dxtech.com/

3DX-Tech. (2017b). *ABS 3D filament.* [Technical Data Sheet]. Retrieved from https://www.3dxtech.com/content/ABS_Filament_v2.1.pdf

3DX-Tech. (2017c). *ABS 3D filament.* [Safety Data Sheet]. Retrieved from http://www.3dxtech.com/content/ABS_SDS_v1.0.pdf

3DX-Tech. (2017d). *CarbonX™ carbon fiber reinforced ABS 3D filament*. [Technical Data Sheet]. Retrieved from https://www.3dxtech.com/content/Carbon_Fiber_ABS_Filament_v2.1.pdf

3DX-Tech. (2017e). *CarbonX™ carbon fiber reinforced ABS 3D filament.* [Safety Data Sheet]. Retrieved from http://www.3dxtech.com/content/CF_ABS_SDS_v1.0.pdf

3DX-Tech. (2017f). *Natural ABS filament.* Retrieved from https://www.3dxtech.com/natural-abs-filament/

3DX-Tech. (2017g). *CarbonX™ carbon fiber ABS 3D-printing filament*. Retrieved from https://www.3dxtech.com/carbonx-carbon-fiber-abs-3d-printing-filament/

Airwolf3D. (2017). *3D-printing filaments*. Retrieved from https://airwolf3d.com/product-category/filament/

ASTM. (2012). *ASTM Standard test method for tensile properties of plastics in D638-03*. 2012. West Conshohocken, PA: ASTM International. Retrieved from www.astm.org

ASTM. (2013). *ASTM Standard test method for melt flow rates of thermoplastics by extrusion in D1238-13*. 2013. West Conshohocken, PA: ASTM International. Retrieved from www.astm.org

Baich, L. (2016). *Impact of infill design on mechanical strength and production cost in material extrusion based additive manufacturing* (Master's thesis). Retrieved from https://etd.ohiolink.edu/!etd.send_file?accession=ysu1485161020020828&disposition=inline

Berman, A. (2007). 3D-printing: making the virtual real. *EDUCAUSE Evolving Technologies Committees,* 1-6. Retrieved from http://www.mvths.org/pages/uploaded_files/DEC0702.pdf

Bhargava, A., Bhargava, A., & Jangid, S. (2014) Fused deposition modeling – An advanced manufacturing methodology. *National Conference on Recent Trends in Mechanical*

Engineering (NCRTME). Jaipur, India. Retrieved from https://www.researchgate.net/publication/266143630_Fused_Deposition_Modeling_-_An_Advanced_Manufacturing

Brooks, G., Kinsley, K., & Owens, T. (2014). 3D printing as a consumer technology business model. *International Journal of Management & Information Systems, 18*(4), 271-280. Retrieved from https://doi.org/10.19030/ijmis.v18i4.8819

Fernandez-Vicente, M., Calle, W., Ferrandiz, S. & Conejero, A. (2016). Effect of infill parameters on tensile mechanical behavior in desktop 3D-printing. *3D-printing and Additive Manufacturing, 3*(3), 183-192. Retrieved from http://online.liebertpub.com/doi/10.1089/3dp.2015.0036 & http://dx.doi.org/10.1089/3dp.2015.0036

Flashforgeusa. (2017). Flashforge Creator Pro. Rowland Heights, CA. Retrieved from http://www.flashforge-usa.com/

Fudali, P., Witkowski, W., & Wydrzyński. (2013). Comparison of geometrical precision of plastic components made by subtractive and additive methods. *Advances in Science and Technology Research Journal, 7*(19), 36-40. Retrieved from http://yadda.icm.edu.pl/baztech/element/bwmeta1.element.baztech-701def13-eab2-498c-865b-d24def1ab733/c/fudali_witkowski.pdf

Ghanbari, D., Salavanti-Niasari, M., Karimzadeh, S. & Gholamrezaei, S. (2014). Hydrothermal synthesis of Bi_2S_3 nanostructures and ABS-based polymeric nanocomposite. *Journal of Nanostructures, 4*, 227-232. Retrieved from http://jns.kashanu.ac.ir/article_7789_f35d05c3ff425c8edcbb7db1b2f262a9.pdf

Goldfein, K., & Slavin, J. (2015). Why sugar is added to food: food science 101. *Journal of Comprehensive Reviews in Food Science and Food Safety, 14*(5), 644-656. Retrieved from http://onlinelibrary.wiley.com/doi/10.1111/1541-4337.12151/abstract & http://dx.doi.org/10.1111/1541-4337.12151

Gururaja, T. R., Shulze, W. A., Cross, L. E., Newnham, R. E., Auld, B. A., & Wang, Y. J. (1985). Piezoelectric composite materials for ultrasonic transducer applications. Part I: Resonant modes of vibration of PZT rod-polymer composites. *IEEE Trans. Sonics Ultrason, 32*(19985), 481-498.

Hashin, Z. (1983). Analysis of composite materials - a survey. *Journal of Applied Mechanics, 50*(3), 481-505. Retrieved from http://appliedmechanics.asmedigitalcollection.asme.org/article.aspx?articleid=1407040

Horton, J. (1989). *U.S. Patent No. 4,876,050 A*. Washington, DC: U.S. Patent and Trademark Office. Retrieved from https://www.google.com/patents/US4876050

Hossain, M. S., Ramos, J., Espalin, D., Perez, M., & Wicker, R. (2013). Improving tensile mechanical properties of FDM-manufactured specimens via modifying build parameters. *International Solid Freeform Fabrication Symposium an Additive Manufacturing Conference*, *2010*, 380-393. Retrieved from https://sffsymposium.engr.utexas.edu/Manuscripts/2013/2013-30-Hossain.pdf

Huang, Q., Zhang, J., Sabbaghi, A., Dasgupta, T., & Epstein, J. D. (2012). Optimal offline compensation of shape shrinkage for 3D-printing processes. *Journal of IISE Transactions, 47*(5), 431-441. Retrieved from http://www.tandfonline.com/doi/abs/10.1080/0740817X.2014.955599?journalCode=uiie20

Huang, X. (2009). Fabrication and properties of carbon fibers. *Chemical Sciences & Materials Systems Laboratory, General Motors Research & Development Center, 2*, 2369-2403. Retrieved from http://www.mdpi.com/1996-1944/2/4/2369/htm

Kumar, B. K. A., Ananthaprasad, M. G., & Krishna, K. G. (2008). A review on corrosion behavior of nickel matrix composites. *International Journal of Emerging Technology and Advanced Engineering, 5*(10), 342-346. Retrieved from https://www.researchgate.net/profile/Anil_Kumar31/publication/283506604_A_Review_on_Corrosion_Behavior_of_Nickel_Matrix_Composites/links/563c269408ae45b5d286af0b.pdf

Kumata, M., Emori, K., Mitsumori, M., Watanabe, H., & Kobayashi, K. (1987). *U.S. Patent No. 4,664,644 A*. Washington, DC: U.S. Patent and Trademark Office. Retrieved from https://www.google.com/patents/US4664644

Lee, T., & Witting, P. (2016). *Computational fluid dynamics (CFD) analysis for off-gas mixing and ventilation inside carbonization furnace during PAN-based carbon fiber manufacturing*. Paper presented at the SAMPE 2016 Conference. Retrieved from http://www.harperintl.com/wp-content/uploads/2011/02/White-Paper-CFD-Analysis-for-Off-gas-mixing-and-ventilation-inside-carbonization-furnace-during-PAN-based-CF-mfg.pdf

Li, J., & Zhang, Y. F. (2009). Tensile strength of ABS/PA6 composites reinforced with HNO_3-treated carbon fibers. *Mechanics of Composite Materials, 45*(5), 537-542. Retrieved from Ebscohost.

Ma, T., Wang, N., Qi, L., & Jia, R. (2014). *Development and application of sheet-like flexible carbon fiber heat-generating element*. Paper presented at the International Conference on Mechatronics, Electronic, Industrial and Control Engineering. Retrieved from http://www.atlantis-press.com/php/download_paper.php?id=15114

Makerbot (2017). *Filament: PLA, ABS, dissolvable, flexible | MakerBot.* New York, NY: Author. Retrieved from https://www.makerbot.com/filament/

Martin, P., Graff, G. L., Gross, M. E., Hall, M., & Mast, E.S. (2005). *U.S. Patent No. 6,962,671.* Washington, DC: U.S. Patent and Trademark Office. Retrieved from https://www.google.com/patents/US6962671

MatWeb. (2017a). *ABS*. Retrieved from www.matweb.com

MatWeb. (2017b). *Overview of materials for acrylonitrile butadiene styrene (ABS), Extruded*. Retrieved from http://www.matweb.com

MatWeb. (2017c). *Sabic cycolac MG94 ABS (Americas)*. Retrieved from http://www.matweb.com

Merrill, E., & Sagar, A. (1995). *U.S. Patent No. 5,459,258 A - Polysaccharide based biodegradable thermoplastic materials.* Washington, DC: U.S. Patent and Trademark Office. Retrieved from https://www.google.com/patents/US5459258

Minus, M., & Kumar, S. (2005). The processing, properties, and structure of carbon fibers. *High Performance Fibers, 57*(2), 52-58. Retrieved from http://dx/doi.org/10.1007/s11837-005-0217-8

Nakagawa, Y., Mori, K., & Maeno, T. (2017). 3D-printing of carbon fibre-reinforced plastic parts. *International Journal of Manufacturing Technology, 91*(5-8), 2811-2817. Retrieved from https://link.springer.com/article/10.1007%2Fs00170-016-9891-7

Ning, F., Cong, W., Qiu, J., Wei, J., & Wang, S. (2015). Additive manufacturing of carbon fiber reinforced thermoplastic composites using fused deposition modeling. *Journal of Composites, 80*, 369-378. Retrieved from http://www.sciencedirect.com/science/article/pii/S1359836815003777

Ning, F., Cong, W., Hu, Y., & Wang, H. (2017). Additive manufacturing of carbon fiber reinforced plastic composites using fused deposition modeling: Effects of process parameters on tensile properties. *Journal of Composite Materials, 51*(4), 451-462. Retrieved from http://dx.doi.org/10.1177/0021998316646169

Novakova-Marcincinova, L., & Kuric, I. (2012). Basic and advanced materials for fused deposition modeling rapid prototyping technology. *Journal of Manufacturing and Industrial Engineering, 11*(1), 24-27. Retrieved from http://www.fvt.tuke.sk/journal/pdf12/1-pp-24-27.pdf

Olivera, S., Muralidhara, H. B., Venkatesh, K., Gopalakrishna, K., & Vivek, C. S. (2016). Plating on acrylonitrile-butadiene-styrene (ABS) plastic: a review. *Journal of Materials Science, 51*(8), 3657-3674. Retrieved from http://dx.doi.org/10.1007%2Fs10853-015-9668-7

Oo-Kuma. (2017). *FDM filaments and granules*. Retrieved from https://www.oo-kuma.com/

Panda, O. (2012). *A study on the effect of fiber parameters on the mechanical behavior of bamboo-glass fiber reinforced epoxy based hybrid composites*. (Master's thesis). Retrieved from http://ethesis.nitrkl.ac.in/3292/1/Ojaswi_Panda_108ME070.pdf

Park, S. (2014). 3D printing industry trends. *International Journal of Advanced Culture Technology, 2*(1), 30-32. Retrieved from http://www.koreascience.or.kr/article/ArticleFullRecord.jsp?cn=E1GMBY_2014_v2n1_30 & http://www.ndsl.kr/soc_img/society/ipact/E1GMBY/2014/v2n1/E1GMBY_2014_v2n1_30.pdf

Rayna, T., & Striukova, L. (2016). From rapid prototyping to home fabrication: How 3D printing is changing business model innovation. *Technological Forecasting & Social Change, 102*, 214-224. Retrieved from http://www.sciencedirect.com/science/article/pii/S0040162515002425?via%3Dihub

Satches, M. (2015). *Nano-composite material development for 3-D printers.* (Master's thesis). Retrieved from https://ttu-ir.tdl.org/ttu-ir/bitstream/handle/2346/66157/SATCHES-THESIS-2015.pdf?sequence=1

Savvakis, K., Petousis, M., Vairis, A., Vidakis, N., & Bikmeyev, A.T. (2014). Experimental determination of the tensile strength of fused deposition modeling parts. *Proceedings of the ASME 2014 International Mechanical Engineering Congress and Exposition*. Retrieved from https://www.researchgate.net/profile/Alexander_Bikmeyev/publication/283498079_Experimental_Determination_of_the_Tensile_Strength_of_Fused_Deposition_Modeling_Parts/links/56d20f0508ae059e375f9ded.pdf

Schaefermeier, P. K., Szymanski, D., Weiss, F., Fu, P., Lueth, T., Schmitz, C., Meiser, B. M., Reichart, B., & Sodian, R. (2009). Design and fabrication of three-dimensional scaffolds for tissue engineering of human heart valves. *Journal of European Surgical Research, 42*(1), 49-53. Retrieved from http://www.karger.com/Article/Abstract/168317

Seong-Mu, J., Sung-Ho, L., Han-ik, J., Se-Joon, P., Hyeon-uk, Y., & Bon-Cheol, K. (2016). *U.S. Patent Application No. 20,160,348,283 A1 - Nanocarbon composite carbon fiber with low cost and high performance and their preparation method*. Washington, DC: U.S. Patent and Trademark Office. Retrieved from https://www.google.com/patents/US20160348283

Sivaraman, P., Chandrasekhar, L., Mishra, V. S., Chakraborta, B. C., & Varghese. (2006). Fracture toughness of thermoplastic co-poly (ether ester) elastomer - Acrylonitrile butadiene styrene terpolymer blend. *Journal of Polymer Testing, 25*(4), 562-567. Retrieved from http://www.sciencedirect.com/science/article/pii/S0142941806000596

Stratasys. (2017). *Materials*. Eden Prairie, MN: Author. Retrieved from http://www.stratasys.com

Tekinalp, H.L., Kunc, V., Velez-Garcia, M.G., Duty, C.E., Love, L.J., Naskar, A.K., Blue, C.A., & Ozcan, S. (2014). Highly oriented carbon fiber-polymer composites via additive manufacturing. *Journal of Composites Science and Technology, 105*, 144-150. Retrieved from http://www.sciencedirect.com/science/article/pii/S0266353814003716

Thakur, P. (2017). *Design for manufacturing and process planning guidelines for improved tensile strength and accuracy of the parts fabricated by 3D-printing* (Master's thesis). Retrieved from http://dspace.thapar.edu:8080/jspui/bitstream/10266/4601/4/4601.pdf

Torrado, A., Roberson, D. A., and Wicker, R.B. (2014). Fracture surface analysis of 3D-printed tensile specimens of novel ABS-based materials. *Journal of Failure Analysis and Prevention, 14*(3), 343-353.

Tymrak, B. M., Kreiger, M., & Pearce, J. M. (2014). Mechanical properties of components fabricated with open-source 3-D printers under realistic environmental conditions. *Materials and Design, 58*(1), 242-246. Retrieved from http://digitalcommons.mtu.edu/cgi/viewcontent.cgi?article=1047&context=materials_fp

Umetani, N., & Schmidt, R. (2013). Cross-sectional structural analysis for 3D-printing optimization. *SIGGRAPH Asia Technical Briefs 2013 Conference proceedings: ACM SIGGRAPH Asia - Technical Briefs Program,* 1-4. Retrieved from https://pdfs.semanticscholar.org/f68c/aa0602d6ce2c3755f7df09569904eb2218eb.pdf

United Calibration Corporation. (2013). *Certificate of calibration*. United Calibration Corp. and United Testing Systems Inc.

Vairis, A., Petousis, M., Vidakis, K., & Savvakis, K. (2016). On the strain rate sensitivity of ABS and ABS Plus fused deposition modeling parts. *Journal of Materials Engineering and Performance, 25*(9), 3558-3565. Retrieved from https://link-springer-com.proxy.bsu.edu/content/pdf/10.1007%2Fs11665-016-2198-x.pdf & http://dx.doi.org/10.1007/s11665-016-2198-x

Vasiliev, V. V., & Morozov, E. V. (2013). *Advanced mechanics of composite materials and structural elements*. The Boulevard, Langford, Kidlington, Oxford: Elsevier Ltd.. Retrieved from https://books.google.com/books?id=T1gRGmoJ9ecC&printsec=frontcover#v=onepage&q&f=false

Walker, J. S. (2014). *Physics*. Upper Saddle River, NJ: Pearson.

Wang, A., & Essner, A. (2002). *U.S. Patent No. 6,414,086 B1*. Washington, DC: U.S. Patent and Trademark Office. Retrieved from https://www.google.com/patents/US6414086

Zoghi, M. (2014). *The International Handbook of FRP Composites in Civil Engineering*. Boca Raton, FL: CRC Press – Taylor & Francis Group. Retrieved from https://books.google.com/books?id=jOHKBQAAQBAJ&pg=PA368&lpg=PA368&dq=%22Carbon+fibers+are+anisotropic+%22&source=bl&ots=J8kyKuJZZU&sig=RKSIMjDpkdFs3945n1KuMNQP9gc&hl=en&sa=X&ved=0ahUKEwiGvqCn7brRAhWj54MKHV7eBQ4Q6AEIGjAA#v=onepage&q=%22Carbon%20fibers%20are%20anisotropic%20%22&f=false

Appendix-A: ASTM D638-02 (2012) Tensile-Test Bone Sample (Type I)

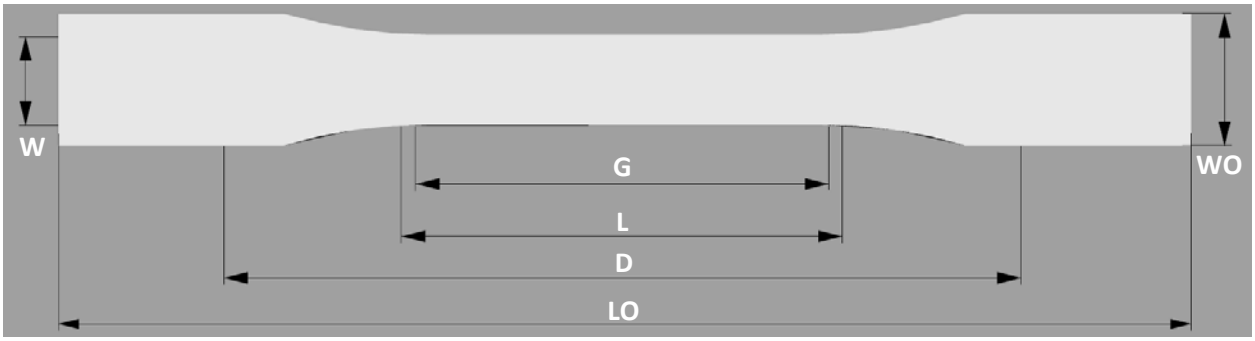

Dimension Abbreviation Titles	Dimension (in (mm))	Tolerances (in (mm))
W - Width of narrow section	.50 (13)	±.02 (±0.5)
L - Length of narrow section	2.25 (57)	±.02 (±0.5)
WO - Width overall	.75 (19)	+.25 (+6.4)
LO - Length Overall	6.5 (165)	no max (no max)
G - Gage length	2 (50)	±.01 (±0.25)
D - Distance between grips	4.5 (115)	±.2 (±5)

"Thickness, T, shall be 3.2 ±0.4 mm (0.13 ±0.02 inch) for all types of molded specimens and for other Types I and II specimens where possible" (ASTM, 2012, p. 49).

Appendix-B: 3DX-Tech (2017b) ABS Material Data Sheet

3DXTECH Technology... Advanced.

Technical Data Sheet
Rev 2.1

3DXTECH® ABS 3D Filament

3DXTECH® ABS [acrylonitrile butadiene styrene] 3D printing filament is formulated utilizing high-flow ABS resin and colorants and then precision extruded using state-of-the-art equipment. ABS is an amorphous polymer with high mechanical and thermal properties – making it the go-to filament for functional prototype and production parts.

3DXTECH® ABS is suitable for use in practically all consumer-grade FDM/FFF printers that have a heated print bed. Made by 3DXTECH® in the USA.

The reported technical data was generated from printed ISO test specimen. The general print parameters utilized are noted below.

- Desktop FDM/FFF Printer
- Nozzle: 0.4mm A2 hardened
- Layer height: 0.2mm
- Infill: 100%, +/- 45°
- Extrusion temp: 230°C
- Bed temp: 110°C
- Bed prep: ABS/Acetone Gel
- Print speed: 50 mm/sec

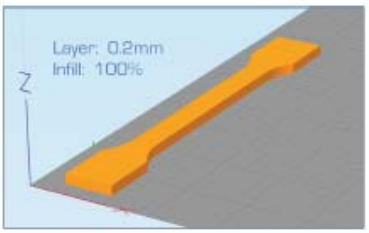

Disclaimer: The technical data contained on this data sheet is furnished without charge or obligation and accepted at the recipient's sole risk. This data should not be used to establish specifications limits or used alone as the basis of design. The data provided is not intended to substitute any testing that may be required to determine fitness for any specific use.

General Property	Unit	Standard	Typical Value
Density	g/cc	ISO 1183	1.05

Mechanical Property	Unit	Standard	Typical Value
Tensile Strength	MPa	ISO 527	41
Tensile Modulus	MPa	ISO 527	1950
Tensile Elongation, Break	%	ISO 527	10
Flexural Modulus	MPa	ISO 178	1983
Flexural Strength	MPa	ISO 178	76

Thermal Property	Unit	Standard	Typical Value
Glass Transition Temperature (Tg)	°C	DSC	105
Heat Distortion Temperature (HDT) @ 0.45MPa	°C	ISO 75	95.9

Electrical Property	Unit	Standard	Typical Value
Surface Resistivity	Ohm/sq	IEC 60093	$>10^{13}$

Printing Recommendation	Typical Range
Extruder Temperature	220 - 240°C
Bed Temperature	100 - 110°C
Print Speed	50 - 70 mm/sec

WWW.3DXTECH.COM

571 Gordon Industrial Court, Suite E
Byron Center, MI 49315 USA

Appendix-C: 3DX-Tech (2017c) ABS Safety Data Sheet

SAFETY DATA SHEET

3DXTECH® ABS

EFFECTIVE DATE: 08 / 01 / 2017 REVISION NUMBER: V1.0

1 PRODUCT AND SUPPLIER INFORMATION

Product Identification:
Product Name: 3DXTECH® ABS
Chemical Name: Acrylonitrile Butadiene Styrene (ABS)

Recommended Use: Additive manufacturing

Supplier Information:
3DXTECH
571 Gordon Industrial Court, Suite E
Byron Center, MI 49315 (USA)
Phone (616) 970-2702
Email: INFO@3DXTECH
Emergency Phone Number: (616) 970-2702

2 HAZARDS INDENTIFICATION

Regulation (EC) NO 1272/2008: Not classified as a dangerous product

Physical Hazards: None

OSHA Regulatory Status: This product is not considered hazardous by the 2012 OSHA Hazard Communication Standard (29 CFR 1910.1200)

3 COMPOSITION/INFORMATION ON INGREDIENTS

Components	CAS No.	Concentration Range (%)
ABS Resin	9003-56-9	100

4 EMERGENCY FIRST AID

Eyes: Flush with water. Consult physician if symptoms persist.

Skin Contact: Wash with soap and water. For thermal burns from molten polymer, immediately flush with cold water. Do not attempt to remove cooled polymer from skin. Obtain medical attention.

Inhalation: Leave exposed area and seek fresh air. If irritation persists seek medical attention.

Ingestion: Not likely due to nature of product. If ingested, drink plenty of water. Do not induce vomiting. Consult a physician if symptoms persist.

5 FIRE AND EXPLOSION HAZARD

Extinguishing Media: Water spray, dry powder, and foam. Carbon dioxide (CO_2)

Safety Precautions for Persons exposed to products of combustion should wear NIOSH approved self contained breathing apparatus and full protective equipment.

Appendix-C: 3DX-Tech (2017c) ABS Safety Data Sheet

6 ACCIDENTAL RELEASE MEASURES

Spill or release: Clean up by vacuuming or sweeping to prevent falls. If molten, allow material to cool and place into an appropriate container for disposal.

7 HANDLING AND STORAGE CONDITIONS

Precautions to be taken in handling and storage: Store in a dry, sprinkler equipped warehouse. Product as shipped is not a combustible dust. Mechanical handling can cause the formation of dusts. To reduce the risk for dust explosion do not permit dust to accumulate.

Waste Disposal: Dispose in accordance with applicable federal, state and local regulations.

8 EXPOSURE AND PROTECTION INFORMATION

Exposure Limits: This product does not contain any hazardous materials with occupational exposure limits established by the region specific regulatory bodies.

Respitory Protection: A NIOSH approved respirator is recommended for protection against processing polymeric fumes, or from dust generated from grinding, sanding, or sawing operations.

Ventilation: Local exhaust is preferred.

Protection Gloves: : Canvas or cotton gloves are recommended.

Eye Protection: Safety glasses with side shields are recommended.

Other: No protective equipment is needed under normal use conditions.

9 PHYSICAL/CHEMICAL DATA

Form: Solid
Appearance: Natural / Ivory
Odor: Slight
Freezing Point: N/A
Solubility in Water: Insoluble
Specific Gravity: >1
% Volatile: N/A
Boiling Range: N/A
Vapor Pressure (MM HG): Negligible
Melting Point: This product does not possess a specific melting point. It softens gradually over a wide temperature range.

Note: Those physical data are typical values based on material tested but may vary from sample to sample. Typical values should not be construed as a guaranteed analysis of any specific lot or as specifications for the product.

10 STABILITY AND REACTIVITY

Polymerization conditions to avoid: None
Chemical Stability: Stable under normal conditions
Conditions to avoid: Incompatible materials, including strong oxidizing agents
Hazardous decomposition byproducts: Thermal decomposition can yield intense heat, dense smoke, phenols, hydrogen cyanide, carbon dioxide, and carbon monoxide.

11 TOXICOLOGICAL INFORMATION

No specific toxicological information is available.

12 ECOLOGICAL INFORMATION

No specific ecological information is available.

Appendix-C: 3DX-Tech (2017c) ABS Safety Data Sheet

13 DISPOSAL

Waste Disposal: Waste or unused product may be discarded in accordance with state, federal, and local regulations.

14 TRANSPORT INFORMATION

Land Transport (DOT): Non-Regulated
Sea Transport (IMDG): Non-Regulated
Air Transport (ICAO/IATA): Non-Regulated

15 REGULATORY INFROMATION

TSCA: Complies
EINECS/ELINCS: N/A
DSL/NDSL: Complies
PICCS: N/A
ENCS: Complies
IECSC: Complies
AICS: Complies
KECL: Complies

16 MISCELLANEOUS INFORMATION

Prepared by: Business Management
Issued: 08/01/2017
Supersedes: N/A

This information set forth herein has been gathered from standard reference materials and/or supplier test data and is, to the best knowledge and belief of 3DXTECH, accurate and reliable. Such information is offered solely for your consideration, investigation and verification, and it is not suggested or guaranteed that the hazard precautions or procedures mentioned are the only ones which exist. 3DXTECH makes no warranties, expressed or implied, with respect to the use of such information or the use of the specific material identified herein combination with any other material or process, and assumes no responsibility therefore.

END OF SDS

Appendix-D: 3DX-Tech (2017d) Carbon Fiber Reinforced ABS Material Data Sheet

3DXTECH Technology... Advanced.

Technical Data Sheet
Rev 2.1

CarbonX™ Carbon Fiber Reinforced ABS 3D Filament

CarbonX™ Carbon Fiber Reinforced ABS (acrylonitrile butadiene styrene terpolymer) is a high-performance carbon fiber reinforced 3D printing filament. This grade was formulated utilizing high-modulus carbon fiber and premium ABS – making it ideal for applications that require superior stiffness, improved dimensional stability and greater thermal resistance than traditional unfilled materials. Suitable for use in practically all consumer-grade FDM/FFF printers that have a heated print bed. Made by 3DXTECH® in the USA.

The reported technical data was generated from printed ISO test specimen. The general print parameters utilized are noted below.

- Desktop FDM/FFF Printer
- Nozzle: 0.4mm A2 hardened
- Layer height: 0.2mm
- Infill: 100%
- Extrusion temp: 230°C
- Bed temp: 110°C
- Bed prep: ABS/Acetone Gel
- Print speed: 50 mm/sec

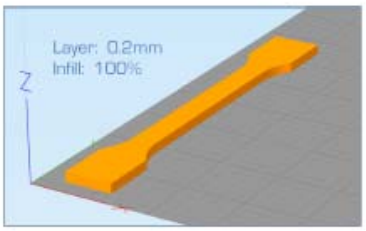

General Property	Unit	Standard	Typical Value
Density	g/cc	ISO 1183	1.11

Mechanical Property	Unit	Standard	Typical Value
Tensile Strength	MPa	ISO 527	44
Tensile Modulus	MPa	ISO 527	4018
Tensile Elongation, Break	%	ISO 527	1.8
Flexural Modulus	MPa	ISO 178	5260
Flexural Strength	MPa	ISO 178	76

Thermal Property	Unit	Standard	Typical Value
Glass Transition Temperature (Tg)	°C	DSC	105
Heat Distortion Temperature (HDT) @ 0.45MPa	°C	ISO 75	102.5

Electrical Property	Unit	Standard	Typical Value
Surface Resistivity	Ohm/sq	IEC 60093	>10^6

Printing Recommendation	Typical Range
Extruder Temperature	220 - 240°C
Bed Temperature	100 - 110°C
Print Speed	50 - 70 mm/sec

WWW.3DXTECH.COM

571 Gordon Industrial Court, Suite E
Byron Center, MI 49315 USA

Appendix-E: 3DX-Tech (2017e) Carbon Fiber Reinforced ABS Safety Data Sheet

SAFETY DATA SHEET

CarbonX™ Carbon Fiber ABS

EFFECTIVE DATE: 08 / 01 / 2017 REVISION NUMBER: V1.0

1 PRODUCT AND SUPPLIER INFORMATION

Product Identification:
Product Name: CarbonX™ CF-ABS
Chemical Name: ABS

Recommended Use: Additive manufacturing

Supplier Information:
3DXTECH
571 Gordon Industrial Court, Suite E
Byron Center, MI 49315 (USA)
Phone (616) 970-2702
Email: INFO@3DXTECH
Emergency Phone Number: (616) 970-2702

2 HAZARDS INDENTIFICATION

Regulation (EC) NO 1272/2008: Not classified as a dangerous product

Physical Hazards: None

OSHA Regulatory Status: This product is not considered hazardous by the 2012 OSHA Hazard Communication Standard (29 CFR 1910.1200)

3 COMPOSITION/INFORMATION ON INGREDIENTS

Components	CAS No.	Concentration Range (%)
ABS Resin	9003-56-9	>80
Carbon Fiber	308063-67-4	<20

4 EMERGENCY FIRST AID

Eyes: Flush with water. Consult physician if symptoms persist.

Skin Contact: Wash with soap and water. For thermal burns from molten polymer, immediately flush with cold water. Do not attempt to remove cooled polymer from skin. Obtain medical attention.

Inhalation: Leave exposed area and seek fresh air. If irritation persists seek medical attention.

Ingestion: Not likely due to nature of product. If ingested, drink plenty of water. Do not induce vomiting. Consult a physician if symptoms persist.

5 FIRE AND EXPLOSION HAZARD

Extinguishing Media: Water spray, dry powder, and foam. Carbon dioxide (CO_2)

Safety Precautions for Persons exposed to products of combustion should wear NIOSH approved self contained breathing apparatus and full protective equipment.

Appendix-E: 3DX-Tech (2017e) Carbon Fiber Reinforced ABS Safety Data Sheet

6 ACCIDENTAL RELEASE MEASURES

Spill or release: Clean up by vacuuming or sweeping to prevent falls. If molten, allow material to cool and place into an appropriate container for disposal.

7 HANDLING AND STORAGE CONDITIONS

Precautions to be taken in handling and storage: Store in a dry, sprinkler equipped warehouse. Product as shipped is not a combustible dust. Mechanical handling can cause the formation of dusts. To reduce the risk for dust explosion do not permit dust to accumulate.

Waste Disposal: Dispose in accordance with applicable federal, state and local regulations.

8 EXPOSURE AND PROTECTION INFORMATION

Exposure Limits: This product does not contain any hazardous materials with occupational exposure limits established by the region specific regulatory bodies.

Respitory Protection: A NIOSH approved respirator is recommended for protection against processing polymeric fumes, or from dust generated from grinding, sanding, or sawing operations.

Ventilation: Local exhaust is preferred.

Protection Gloves: : Canvas or cotton gloves are recommended.

Eye Protection: Safety glasses with side shields are recommended.

Other: No protective equipment is needed under normal use conditions.

9 PHYSICAL/CHEMICAL DATA

Form: Solid
Appearance: Black Filament
Odor: Slight
Freezing Point: N/A
Solubility in Water: Insoluble
Specific Gravity: >1
% Volatile: N/A
Boiling Range: N/A
Vapor Pressure [MM HG]: Negligible
Melting Point: This product does not possess a specific melting point. It softens gradually over a wide temperature range.

Note: Those physical data are typical values based on material tested but may vary from sample to sample. Typical values should not be construed as a guaranteed analysis of any specific lot or as specifications for the product.

10 STABILITY AND REACTIVITY

Polymerization conditions to avoid: None
Chemical Stability: Stable under normal conditions
Conditions to avoid: Incompatible materials, including strong oxidizing agents
Hazardous decomposition byproducts: Thermal decomposition can yield intense heat, dense smoke, phenols, hydrogen cyanide, carbon dioxide, and carbon monoxide.

11 TOXICOLOGICAL INFORMATION

No specific toxicological information is available.

12 ECOLOGICAL INFORMATION

No specific ecological information is available.

Appendix-E: 3DX-Tech (2017e) Carbon Fiber Reinforced ABS Safety Data Sheet

13 DISPOSAL

Waste Disposal: Waste or unused product may be discarded in accordance with state, federal, and local regulations.

14 TRANSPORT INFORMATION

Land Transport (DOT): Non-Regulated
Sea Transport (IMDG): Non-Regulated
Air Transport (ICAO/IATA): Non-Regulated

15 REGULATORY INFROMATION

TSCA: Complies
EINECS/ELINCS: N/A
DSL/NDSL: Complies
PICCS: N/A
ENCS: Complies
IECSC: Complies
AICS: Complies
KECL: Complies

16 MISCELLANEOUS INFORMATION

Prepared by: Business Management
Issued: 08/01/2017
Supersedes: N/A

This information set forth herein has been gathered from standard reference materials and/or supplier test data and is, to the best knowledge and belief of 3DXTECH, accurate and reliable. Such information is offered solely for your consideration, investigation and verification, and it is not suggested or guaranteed that the hazard precautions or procedures mentioned are the only ones which exist. 3DXTECH makes no warranties, expressed or implied, with respect to the use of such information or the use of the specific material identified herein combination with any other material or process, and assumes no responsibility therefore.

END OF SDS

Appendix-F: Matweb (2007) Sabic Cycolac MG94 ABS (Americas)

Physical Properties	Metric	English	Comments
Specific Gravity	1.05 g/cc	1.05 g/cc	ASTM D 792
Density	1.04 g/cc	0.0376 lb/in³	ISO 1183
Viscosity	172000 cP @Shear Rate 100 1/s, Temperature 240 °C	172000 cP @Shear Rate 100 1/s, Temperature 464 °F	Melt; ASTM D 3825
Linear Mold Shrinkage, Flow	0.0050 - 0.0080 cm/cm @Thickness 3.20 mm	0.0050 - 0.0080 in/in @Thickness 0.126 inch	SABIC Method
Melt Flow	11.7 g/10 min @Load 3.80 kg, Temperature 230 °C	11.7 g/10 min @Load 8.38 lb, Temperature 446 °F	ASTM D 1238
	12 g/10 min @Load 5.00 kg, Temperature 220 °C	12 g/10 min @Load 11.0 lb, Temperature 428 °F	ISO 1133
	42 g/10 min @Load 10.0 kg, Temperature 220 °C	42 g/10 min @Load 22.0 lb, Temperature 428 °F	ISO 1133

Appendix-G: Simplify3D (2017) Settings Kept Default for 3D-printing Specimens

- Extrusion Speed: 3600.0 mm/min
- Outline Underspeed: 50%
- Solid Infill Underspeed: 80%
- Support Structure Underspeed: 80%
- X/Y Axis Movement Speed: 4800.0 mm/min
- Z Axis Movement Speed: 1000.0 mm/min
- Retraction Distance: 1.00 mm
- Extra Restart Distance: 0.00 mm
- Retraction Vertical Lift: 0.00 mm
- Retraction Speed: 1800.0 mm/min
- Coasting at the end was not selected (with a check mark in this case).
- Nozzle Wipe not selected but was included in the script (with a check-mark in this case).
- Layer Height: .2000 mm
- Outline/Perimeter Shells: 2
- Outline Direction: Inside-Out
- Sequential island and corkscrew printing were not selected (with a check-mark in this case).
- First Layer Width: 100%
- First Layer Speed: 50%
- Optimizing start points for fastest printing speed was selected.
- No skirts, rafts, pillars, or ooze shields were selected (with a check-mark in this case).
- Internal Fill Pattern was Rectilinear; however, due to Interior Fill Percentage being moved to 100% as specified earlier.
- Outline Overlap: 15%
- Infill Extrusion Width: 100%
- Minimum Infill Length: 5.00 mm
- Combine Infill Every: 1 layer
- Including a solid diaphragm per a specified number of layers is not selected (with a check-mark in this case).

Appendix-G: Simplify3D (2017) Settings Kept Default for 3D-printing Specimens

- External Infill Angle Offsets set to ±45 degrees; however, does not apply to the 3D-prints in this study.
- Generating support material is not selected (with a check-mark in this case).
- Waiting for the temperature controller to stabilize before beginning the build is not selected (with a check-mark in this case).
- Cooling fans were not used.
- 5D firmware (include E-Dimension), Allow zeroing of extrusion distances (i.e., G92 E0), and Firmware supports "stick" parameters were each selected (with a check-mark in this case).
- Relative extrusion distances, using independent extruder axes, including M101/M102/M103 commands, and applying toolhead offsets to G-code coordinates are not selected (with a check-mark in this case).
- Global G-code Offsets were each set to 0.00.
- Filament Toolhead Index: Tool 0 (with a drop-down menu in this case).
- Filament Diameter: 1.7500 mm
- Filament Price: 46.00 price/kg
- Filament density 1.25 grams/cm^3
- Tool change settings were not needed in this study.
- Only retracting when crossing open spaces, forcing retraction between layers, and wiping extruder for outer-most perimeters were selected (with the use of check-marks in this case); however, these did not apply to the study.
- Minimum travel for retraction and performing retraction during wiping movements were not selected (with the use of check-marks in this case).
- The slicing behavior for non-manifold segments was set to "heal" and merging all outlines into a single solid model were not selected (with the use of check-marks in this case); however, these did not apply to the study.

Appendix-H: Record-Keeping

ASTM D638-02a Tensile Testing Records for Thesis Research

Material 1 Identification	Material 2 Identification
Material: ABS	Material: Carbon Fiber Loaded/Reinforced ABS
Type: Unknown	Type: ABS is Sabic MG-94; Carbon is unknown
Source: 3DX-Tech	Source: 3DX-Tech
Manufactuer's Numbers: SKU-F9716F06	Manufacturers Numbers: SKU-C6E11CF9
Form: Filament to 3D-printed Specimens	Form: Filament to 3D-Printed Specimens
Principal Dimentions: Type 1 ASTM Requirments	Principal Dimentions: Type 1 ASTM Requirments
Previous history: Virgin Mateiral	Previous history: Virgin Material

Date Testing Occurred: October 13, 2017
Revision Date of Test Method D638: 02
Method of preparing test specimens: 3D-Printed
Conditioning Procedure Used:
Atmospheric conditions: ~73 degrees Farenheight, uncontrolled. Humidity unknown.
Number of specimens tested: 180
Speed of Testing: .2 in/min
Classification of extensometer used
Average Overall Length of all samples: 165mm +/- .5mm
Average Overall Width of all samples: 19mm +/- 6.4mm
Average Overall Length of the narrow section of all samples: 57mm +/- .5mm
Refer to Code Book In Appendix-H for abbreviationon-explanations regarding this sheet
: Entered into machine software as specimen size due to being lowest recorded value

ID#	Material	W1	W2	W3	T1	T2	T3	T Sth Y	T Sth B	T Stn Y	T Stn B	% E	% E Y	% E B	M	Mass	Comments
A1-15	ABS	0.514	0.513	0.514	0.124	0.124	0.123	3,457.56	6,835.59	218.17	431.33	1.00	0.99	7.68	366,768.00	7.93	Good Break
A2-15	ABS	0.516	0.512	0.513	0.123	0.123	0.124	6,674.56	6,830.26	420.50	430.31	1.00	1.00	6.79	360,614.00	7.89	Good Break
A3-15	ABS	0.518	0.513	0.514	0.123	0.123	0.123	3,738.03	6,911.21	235.87	436.10	1.00	0.98	7.15	374,969.00	7.92	Good Break
A4-15	ABS	0.516	0.511	0.514	0.124	0.123	0.123	3,591.62	6,825.39	225.91	429.32	1.00	0.99	6.91	380,523.00	7.9	Good Break
A5-15	ABS	0.515	0.512	0.513	0.123	0.123	0.123	6,683.00	6,925.00	421.03	436.27	1.00	1.00	6.83	374,621.00	7.94	Good Break
A6-15	ABS	0.516	0.513	0.514	0.124	0.124	0.123	6,797.20	6,853.15	428.90	432.43	1.00	1.00	6.84	377,285.00	7.93	Good Break
A7-15	ABS	0.516	0.513	0.514	0.124	0.123	0.123	3,600.37	6,912.62	227.18	436.19	1.00	0.99	7.64	371,603.00	7.93	Good Break
A8-15	ABS	0.516	0.512	0.512	0.123	0.123	0.124	3,621.80	6,905.30	228.17	435.03	1.00	0.98	6.75	386,542.00	7.95	Good Break
A9-15	ABS	0.517	0.512	0.512	0.123	0.123	0.123	3,697.30	6,879.97	232.93	433.44	1.00	0.99	6.78	382,694.00	7.93	Good Break
A10-15	ABS	0.518	0.516	0.517	0.123	0.123	0.123	3,566.52	6,788.81	226.47	431.09	1.00	0.98	6.81	383,361.00	7.9	Good Break
A11-15	ABS	0.518	0.515	0.516	0.124	0.124	0.123	3,672.57	6,878.98	232.84	436.13	1.00	0.99	6.76	382,897.00	7.91	Good Break
A12-15	ABS	0.518	0.513	0.516	0.123	0.123	0.123	6,785.26	6,831.38	428.15	431.06	1.00	1.00	7.10	388,585.00	7.91	Good Break
A13-15	ABS	0.518	0.512	0.513	0.124	0.123	0.123	3,709.26	6,841.75	233.68	431.03	1.00	0.98	6.73	390,606.00	7.94	Good Break
A14-15	ABS	0.516	0.514	0.515	0.123	0.123	0.123	6,713.75	6,846.51	424.31	432.70	1.00	1.00	6.67	371,764.00	7.9	Good Break
A15-15	ABS	0.518	0.514	0.516	0.124	0.123	0.124	3,663.16	6,816.60	231.51	430.81	1.00	0.99	6.61	377,664.00	7.9	Good Break
A1-30	ABS	0.517	0.511	0.511	0.124	0.124	0.124	3,200.04	5,839.99	202.88	370.26	1.00	0.98	12.76	330,113.00	7.84	Good Break
A2-30	ABS	0.513	0.511	0.514	0.123	0.123	0.124	3,327.64	5,774.15	209.31	363.19	1.00	0.99	9.74	344,745.00	7.8	Good Break
A3-30	ABS	0.517	0.512	0.513	0.124	0.124	0.124	3,217.34	5,870.58	204.30	372.78	1.00	0.98	7.84	353,112.00	7.86	Good Break
A4-30	ABS	0.518	0.511	0.511	0.123	0.123	0.124	3,257.89	5,940.67	204.92	373.67	1.00	0.98	8.63	329,619.00	7.84	Good Break
A5-30	ABS	0.514	0.511	0.511	0.124	0.124	0.124	3,269.94	5,799.45	207.31	367.69	1.00	0.99	9.08	343,336.00	7.81	Good Break
A6-30	ABS	0.515	0.512	0.515	0.123	0.123	0.123	3,286.48	5,943.43	207.05	374.44	1.00	0.98	10.79	339,777.00	7.86	Good Break
A7-30	ABS	0.515	0.511	0.511	0.124	0.124	0.124	3,348.00	5,801.55	212.26	367.82	1.00	0.99	8.17	344,227.00	7.86	Good Break
A8-30	ABS	0.516	0.512	0.515	0.123	0.123	0.124	5,897.94	5,906.38	371.57	372.10	1.00	1.00	11.36	344,871.00	7.87	Good Break
A9-30	ABS	0.516	0.511	0.513	0.124	0.123	0.124	3,612.05	5,941.14	227.20	373.70	1.00	0.98	7.68	355,839.00	7.89	Good Break
A10-30	ABS	0.513	0.511	0.512	0.123	0.123	0.124	3,283.02	5,879.84	206.50	369.84	1.00	0.98	9.67	340,103.00	7.84	Good Break
A11-30	ABS	0.515	0.512	0.513	0.124	0.123	0.124	3,264.44	5,904.04	205.66	371.95	1.00	0.98	11.48	341,651.00	7.86	Good Break
A12-30	ABS	0.517	0.511	0.511	0.124	0.124	0.124	3,184.43	5,760.07	201.89	365.19	1.00	0.98	8.99	332,004.00	7.85	Good Break
A13-30	ABS	0.517	0.513	0.513	0.124	0.123	0.123	6,006.35	6,007.99	379.00	379.10	1.00	1.00	11.46	339,750.00	7.88	Good Break
A14-30	ABS	0.518	0.514	0.516	0.123	0.123	0.123	5,910.83	5,927.19	373.56	374.60	1.00	1.00	8.56	344,965.00	7.85	Good Break
A15-30	ABS	0.516	0.511	0.513	0.124	0.124	0.123	3,273.63	5,872.56	205.91	369.38	1.00	0.98	7.68	336,841.00	7.83	Good Break
A1-45	ABS	0.516	0.511	0.514	0.123	0.123	0.123	3,124.96	5,241.02	196.56	329.66	1.00	0.98	8.31	333,910.00	7.84	Good Break
A2-45	ABS	0.516	0.511	0.511	0.123	0.123	0.124	3,051.92	5,241.49	191.97	329.69	1.00	0.98	10.65	327,345.00	7.87	Good Break
A3-45	ABS	0.515	0.519	0.511	0.124	0.124	0.124	5,995.41	5,995.41	380.11	380.11	1.00	1.00	9.29	371,697.00	8.19	Good Break
A4-45	ABS	0.514	0.514	0.514	0.121	0.121	0.121	6,427.19	6,493.69	399.77	403.91	1.00	1.00	6.31	375,525.00	8.1	Good Break
A5-45	ABS	0.516	0.511	0.512	0.123	0.123	0.122	6,135.84	6,135.84	385.94	385.94	1.00	1.00	6.84	363,481.00	8.13	Good Break

Appendix-H: Record-Keeping

A6-45	ABS	0.514	0.511	0.511	0.124	0.124	0.124	3,082.14	5,231.85	195.41	331.70	1.00	0.99	8.28	323,597.00	7.89	Good Break
A7-45	ABS	0.517	0.51	0.512	0.124	0.123	0.123	5,294.26	5,299.68	331.95	332.29	1.00	1.00	8.54	341,191.00	7.86	Good Break
A8-45	ABS	0.518	0.519	0.511	0.124	0.124	0.124	3,025.06	5,244.89	191.79	332.53	1.00	0.98	7.48	338,209.00	7.91	Good Break
A9-45	ABS	0.516	0.519	0.511	0.124	0.124	0.124	5,323.42	5,327.15	337.50	337.74	1.00	1.00	8.69	335,383.00	7.94	Good Break
A10-45	ABS	0.511	0.518	0.511	0.125	0.125	0.124	3,036.24	5,276.12	192.50	334.51	1.00	0.98	9.49	322,658.00	7.92	Good Break
A11-45	ABS	0.516	0.519	0.512	0.125	0.124	0.124	3,112.65	5,290.84	197.65	335.97	1.00	0.99	7.21	322,537.00	7.9	Good Break
A12-45	ABS	0.515	0.519	0.511	0.124	0.124	0.124	3,032.05	5,244.66	192.23	332.51	1.00	0.98	7.75	331,632.00	7.89	Good Break
A13-45	ABS	0.512	0.518	0.511	0.125	0.124	0.124	5,150.06	5,151.46	326.51	326.60	1.00	1.00	8.69	313,563.00	7.89	Good Break
A14-45	ABS	0.513	0.519	0.511	0.124	0.124	0.125	5,117.21	5,117.21	324.43	324.43	1.00	1.00	6.99	318,970.00	7.86	Good Break
A15-45	ABS	0.517	0.514	0.512	0.12	0.12	0.12	3,743.84	6,687.29	229.87	410.60	1.00	0.98	7.02	394,140.00	8.1	Good Break
A1-60	ABS	0.515	0.514	0.516	0.12	0.119	0.119	3,245.80	5,445.26	198.64	333.25	1.00	0.98	6.12	343,875.00	7.7	Good Break
A2-60	ABS	0.514	0.511	0.51	0.124	0.124	0.123	2,751.84	4,526.42	172.54	283.81	1.00	0.99	6.78	298,196.00	7.74	Good Break
A3-60	ABS	0.51	0.51	0.519	0.123	0.123	0.124	2,761.73	4,449.14	173.16	278.96	1.00	0.98	5.61	294,152.00	7.73	Good Break
A4-60	ABS	0.512	0.51	0.513	0.123	0.123	0.123	2,945.27	4,767.68	184.67	298.93	1.00	0.98	6.53	315,593.00	7.83	Good Break
A5-60	ABS	0.51	0.51	0.519	0.123	0.123	0.124	2,871.29	4,611.94	180.03	289.17	1.00	0.98	5.79	314,163.00	7.79	Good Break
A6-60	ABS	0.513	0.513	0.514	0.122	0.122	0.122	2,973.81	4,759.01	186.16	297.91	1.00	0.98	6.84	317,751.00	7.78	Good Break
A7-60	ABS	0.515	0.519	0.519	0.123	0.124	0.124	2,874.54	4,494.38	182.25	284.94	1.00	0.98	5.34	301,857.00	7.79	Good Break
A8-60	ABS	0.511	0.519	0.519	0.124	0.124	0.124	2,813.26	4,511.16	178.36	286.01	1.00	0.98	5.93	301,909.00	7.81	Good Break
A9-60	ABS	0.514	0.518	0.518	0.124	0.124	0.124	2,722.09	4,333.38	173.40	276.04	1.00	0.99	5.82	294,375.00	7.79	Good Break
A10-60	ABS	0.516	0.51	0.51	0.124	0.123	0.123	2,867.75	4,529.48	179.81	284.00	1.00	0.98	5.90	306,978.00	7.81	Good Break
A11-60	ABS	0.511	0.518	0.517	0.124	0.124	0.124	2,744.99	4,397.92	174.03	278.83	1.00	0.98	6.66	285,337.00	7.77	Good Break
A12-60	ABS	0.51	0.517	0.517	0.124	0.124	0.124	2,730.07	4,379.11	172.54	276.76	1.00	0.98	5.57	301,876.00	7.78	Good Break
A13-60	ABS	0.512	0.517	0.519	0.125	0.124	0.124	2,635.51	4,337.48	167.36	275.43	1.00	0.98	5.94	292,783.00	7.78	Good Break
A14-60	ABS	0.512	0.517	0.519	0.125	0.124	0.124	2,671.34	4,304.92	169.63	273.36	1.00	0.98	5.78	292,939.00	7.77	Good Break
A15-60	ABS	0.513	0.518	0.519	0.125	0.124	0.124	2,755.40	4,443.55	175.24	282.61	1.00	0.98	6.07	306,050.00	7.83	Good Break
A1-75	ABS	0.511	0.518	0.518	0.125	0.124	0.125	2,678.11	4,146.97	169.79	262.92	1.00	0.98	4.77	318,519.00	7.83	Good Break
A2-75	ABS	0.512	0.518	0.519	0.124	0.123	0.123	2,693.48	4,163.22	169.69	262.28	1.00	0.98	4.45	298,717.00	7.82	Good Break
A3-75	ABS	0.519	0.517	0.519	0.125	0.124	0.124	2,674.91	3,939.21	171.46	252.50	1.00	0.98	4.15	301,687.00	7.85	Good Break
A4-75	ABS	0.513	0.517	0.519	0.124	0.124	0.124	2,712.66	4,092.12	172.53	260.26	1.00	0.98	4.22	306,462.00	7.83	Good Break
A5-75	ABS	0.512	0.518	0.51	0.124	0.124	0.125	2,661.58	4,007.23	168.21	253.26	1.00	0.98	4.35	290,907.00	7.81	Good Break
A6-75	ABS	0.514	0.517	0.51	0.125	0.125	0.124	2,666.49	4,051.17	168.52	256.03	1.00	0.97	4.40	303,757.00	7.83	Good Break
A7-75	ABS	0.511	0.517	0.51	0.125	0.125	0.124	2,758.11	4,051.64	174.31	256.06	1.00	0.98	3.99	294,811.00	7.84	Good Break
A8-75	ABS	0.511	0.518	0.519	0.124	0.125	0.124	2,649.46	3,999.25	167.98	253.55	1.00	0.98	4.28	289,798.00	7.85	Good Break
A9-75	ABS	0.511	0.517	0.51	0.125	0.125	0.125	2,467.75	3,803.99	157.44	242.69	1.00	0.98	4.53	281,785.00	7.84	Good Break
A10-75	ABS	0.511	0.517	0.51	0.124	0.124	0.124	2,668.12	4,115.68	168.63	260.11	1.00	0.98	4.44	301,276.00	7.84	Good Break
A11-75	ABS	0.513	0.518	0.519	0.125	0.124	0.124	2,684.79	4,140.90	170.75	263.36	1.00	0.98	4.63	298,876.00	7.85	Good Break

Appendix-H: Record-Keeping

A12-75	ABS	0.512	0.518	0.511	0.125	0.124	0.124	2,721.92	4,051.91	172.57	256.89	1.00	0.98	4.31	314,218.00	7.85	Good Break
A13-75	ABS	0.514	0.518	0.519	0.124	0.124	0.124	2,602.89	3,865.15	165.80	246.21	1.00	0.98	3.85	298,122.00	7.81	Good Break
A14-75	ABS	0.513	0.518	0.51	0.125	0.125	0.125	2,661.56	3,986.68	169.81	254.35	1.00	0.98	4.28	298,717.00	7.83	Good Break
A15-75	ABS	0.512	0.518	0.519	0.124	0.124	0.124	2,641.56	3,925.48	167.74	249.27	1.00	0.98	4.18	289,355.00	7.8	Good Break
A1-90	ABS	0.513	0.51	0.51	0.124	0.123	0.124	3,181.11	5,053.94	199.46	316.88	1.00	0.99	4.28	340,071.00	7.83	Good Break
A2-90	ABS	0.513	0.512	0.511	0.123	0.124	0.125	3,248.26	5,176.91	204.32	325.63	1.00	0.99	4.26	347,897.00	7.84	Good Break
A3-90	ABS	0.511	0.51	0.51	0.125	0.124	0.125	4,735.57	5,105.82	299.29	322.69	1.00	1.00	4.51	334,129.00	7.86	Good Break
A4-90	ABS	0.514	0.515	0.517	0.12	0.118	0.118	5,414.67	5,935.73	328.67	360.30	1.00	1.00	4.80	377,182.00	7.71	Good Break
A5-90	ABS	0.515	0.513	0.513	0.123	0.121	0.122	5,037.59	5,455.79	312.83	338.80	1.00	1.00	4.66	347,105.00	7.81	Good Break
A6-90	ABS	0.513	0.519	0.518	0.125	0.124	0.125	3,132.14	5,108.32	199.20	324.89	1.00	0.99	4.49	340,967.00	7.88	Good Break
A7-90	ABS	0.511	0.519	0.518	0.125	0.124	0.125	3,200.28	5,122.80	202.90	324.79	1.00	0.99	4.30	339,876.00	7.91	Good Break
A8-90	ABS	0.513	0.51	0.51	0.124	0.124	0.125	4,732.77	5,176.18	299.11	327.13	1.00	1.00	4.36	342,711.00	7.89	Good Break
A9-90	ABS	0.513	0.519	0.51	0.126	0.124	0.125	3,202.69	5,025.18	202.41	317.59	1.00	0.98	4.05	336,431.00	7.87	Good Break
A10-90	ABS	0.513	0.518	0.519	0.126	0.124	0.123	3,241.95	5,190.70	204.57	327.53	1.00	0.98	4.24	343,641.00	7.87	Good Break
A11-90	ABS	0.514	0.511	0.513	0.124	0.123	0.124	4,690.52	5,218.71	295.03	328.26	1.00	1.00	4.23	340,775.00	7.84	Good Break
A12-90	ABS	0.514	0.51	0.519	0.123	0.124	0.124	3,337.08	5,143.94	209.23	322.53	1.00	0.98	4.09	355,607.00	7.87	Good Break
A13-90	ABS	0.511	0.517	0.516	0.125	0.125	0.126	3,041.61	4,906.32	194.36	313.51	1.00	0.98	4.35	326,698.00	7.84	Good Break
A14-90	ABS	0.513	0.51	0.519	0.125	0.124	0.125	3,193.57	5,118.44	201.83	323.49	1.00	0.98	4.24	340,417.00	7.87	Good Break
A15-90	ABS	0.514	0.51	0.519	0.125	0.124	0.124	3,178.38	5,060.71	200.87	319.84	1.00	0.98	4.23	355,380.00	7.84	Good Break
CF1-15	CF-ABS	0.515	0.516	0.517	0.124	0.125	0.124	5,665.95	6,533.58	357.52	412.27	1.00	0.97	2.26	755,647.00	8.28	Good Break
CF2-15	CF-ABS	0.518	0.518	0.518	0.123	0.123	0.122	5,750.02	6,520.21	363.40	412.08	1.00	0.97	2.29	818,979.00	8.24	Good Break
CF3-15	CF-ABS	0.516	0.514	0.514	0.123	0.124	0.122	6,139.86	6,743.96	384.97	422.85	1.00	0.96	1.91	892,109.00	8.31	Good Break
CF4-15	CF-ABS	0.514	0.512	0.512	0.123	0.123	0.123	5,964.07	6,587.33	375.74	415.00	1.00	0.97	1.89	853,439.00	8.3	Good Break
CF5-15	CF-ABS	0.515	0.514	0.515	0.123	0.122	0.122	5,595.37	6,581.39	350.83	412.65	1.00	0.97	2.35	727,224.00	8.31	Good Break
CF6-15	CF-ABS	0.517	0.514	0.514	0.123	0.123	0.124	6,163.98	6,823.14	389.56	431.22	1.00	0.97	2.13	894,662.00	8.36	Good Break
CF7-15	CF-ABS	0.514	0.514	0.514	0.124	0.122	0.122	5,902.13	6,453.46	370.06	404.63	1.00	0.95	2.06	918,067.00	8.34	Good Break
CF8-15	CF-ABS	0.512	0.513	0.512	0.123	0.123	0.122	5,776.13	6,257.36	361.01	391.09	1.00	0.96	1.98	812,748.00	8.32	Good Break
CF9-15	CF-ABS	0.517	0.512	0.512	0.124	0.124	0.123	5,836.04	6,575.61	367.67	414.26	1.00	0.96	2.14	853,303.00	8.39	Good Break
CF10-15	CF-ABS	0.517	0.513	0.513	0.123	0.123	0.122	5,739.53	6,509.78	359.29	407.51	1.00	0.97	2.09	803,581.00	8.3	Good Break
CF11-15	CF-ABS	0.514	0.512	0.512	0.123	0.123	0.123	5,755.14	6,444.77	362.57	406.02	1.00	0.96	1.96	807,476.00	8.37	Good Break
CF12-15	CF-ABS	0.515	0.514	0.514	0.123	0.123	0.123	5,814.76	6,516.93	367.49	411.87	1.00	0.96	2.14	834,275.00	8.35	Good Break
CF13-15	CF-ABS	0.517	0.514	0.515	0.122	0.122	0.122	5,608.09	6,519.19	351.63	408.75	1.00	0.97	2.30	707,156.00	8.28	Good Break
CF14-15	CF-ABS	0.517	0.514	0.514	0.123	0.122	0.122	5,704.93	6,562.07	357.70	411.44	1.00	0.97	2.15	770,963.00	8.33	Good Break
CF15-15	CF-ABS	0.515	0.514	0.514	0.124	0.123	0.123	5,631.28	5,758.43	355.90	363.93	1.00	0.96	1.61	784,907.00	8.26	Good Break
CF1-30	CF-ABS	0.514	0.511	0.513	0.124	0.123	0.123	4,446.97	5,413.65	279.71	340.52	1.00	0.97	2.81	576,697.00	8.22	Good Break
CF2-30	CF-ABS	0.518	0.517	0.518	0.125	0.125	0.124	4,218.53	5,182.78	270.41	332.22	1.00	0.97	3.14	550,990.00	8.2	Good Break

Appendix-H: Record-Keeping

CF3-30	CF-ABS	0.511	0.519	0.519	0.126	0.125	0.125	4,337.84	5,295.40	277.19	338.38	1.01	0.97	2.97	573,341.00	8.22	Good Break
CF4-30	CF-ABS	0.512	0.51	0.51	0.125	0.124	0.124	4,388.93	5,343.54	277.38	337.71	1.00	0.97	3.01	569,664.00	8.23	Good Break
CF5-30	CF-ABS	0.512	0.519	0.51	0.124	0.124	0.124	4,371.87	5,235.78	276.30	330.90	1.00	0.97	2.39	579,716.00	8.2	Good Break
CF6-30	CF-ABS	0.519	0.51	0.519	0.125	0.123	0.123	4,686.39	5,623.88	293.84	352.62	1.00	0.97	2.91	621,869.00	8.32	Good Break
CF7-30	CF-ABS	0.514	0.512	0.512	0.124	0.123	0.123	4,643.44	5,569.90	292.54	350.90	1.00	0.97	2.91	620,114.00	8.28	Good Break
CF8-30	CF-ABS	0.513	0.51	0.51	0.124	0.123	0.123	4,516.05	5,425.26	283.16	340.16	1.00	0.97	2.89	604,128.00	8.24	Good Break
CF9-30	CF-ABS	0.51	0.518	0.519	0.126	0.125	0.124	4,419.32	5,388.18	279.30	340.53	1.00	0.97	2.98	572,225.00	8.25	Good Break
CF10-30	CF-ABS	0.511	0.518	0.518	0.126	0.125	0.126	4,363.74	5,327.31	278.84	340.41	1.00	0.96	3.00	610,318.00	8.28	Good Break
CF11-30	CF-ABS	0.515	0.514	0.515	0.123	0.122	0.122	4,519.82	5,493.59	283.39	344.45	1.00	0.97	2.63	566,063.00	8.24	Good Break
CF12-30	CF-ABS	0.511	0.519	0.519	0.125	0.124	0.124	4,334.31	5,274.95	274.80	334.43	1.00	0.97	3.05	588,589.00	8.21	Good Break
CF13-30	CF-ABS	0.513	0.513	0.512	0.123	0.123	0.124	4,383.17	5,485.25	276.14	345.57	1.00	0.97	3.38	542,745.00	8.23	Good Break
CF14-30	CF-ABS	0.512	0.512	0.512	0.124	0.123	0.123	4,606.40	5,574.35	290.20	351.18	1.00	0.97	3.04	567,409.00	8.3	Good Break
CF15-30	CF-ABS	0.512	0.514	0.512	0.123	0.122	0.122	4,656.01	5,675.67	291.00	354.73	1.00	0.96	2.94	627,987.00	8.3	Good Break
CF1-45	CF-ABS	0.515	0.514	0.512	0.124	0.123	0.124	3,726.14	4,907.24	234.75	309.16	1.00	0.98	3.53	432,433.00	8.27	Good Break
CF2-45	CF-ABS	0.518	0.518	0.519	0.12	0.119	0.118	4,240.46	5,472.07	259.09	334.34	1.00	0.98	3.30	524,786.00	8.13	Good Break
CF3-45	CF-ABS	0.518	0.517	0.518	0.12	0.12	0.121	4,057.39	5,236.09	251.56	324.64	1.00	0.97	3.82	499,438.00	8.07	Good Break
CF4-45	CF-ABS	0.516	0.513	0.513	0.124	0.125	0.124	3,539.78	4,692.31	225.13	298.43	1.00	0.97	3.63	436,120.00	8.07	Good Break
CF5-45	CF-ABS	0.516	0.511	0.512	0.125	0.124	0.126	3,625.51	4,661.91	229.86	295.57	1.00	0.97	4.02	471,417.00	8.13	Good Break
CF6-45	CF-ABS	0.515	0.515	0.515	0.125	0.124	0.124	3,818.61	4,874.42	244.01	311.48	1.00	0.97	3.07	477,784.00	8.22	Good Break
CF7-45	CF-ABS	0.517	0.516	0.515	0.123	0.123	0.123	4,096.88	5,097.87	259.74	323.20	1.00	0.97	3.34	485,508.00	8.24	Good Break
CF8-45	CF-ABS	0.517	0.517	0.518	0.125	0.123	0.123	4,057.51	4,989.16	258.06	317.31	1.00	0.97	2.69	505,115.00	8.24	Good Break
CF9-45	CF-ABS	0.516	0.511	0.512	0.125	0.125	0.126	3,835.02	4,972.44	245.06	317.74	1.00	0.97	3.72	483,467.00	8.24	Good Break
CF10-45	CF-ABS	0.517	0.513	0.514	0.125	0.124	0.124	4,035.45	5,134.10	256.65	326.53	1.00	0.97	4.21	511,586.00	8.3	Good Break
CF11-45	CF-ABS	0.513	0.51	0.51	0.125	0.125	0.125	3,956.40	5,092.01	249.25	320.80	1.00	0.97	3.05	503,036.00	7.79	Good Break
CF12-45	CF-ABS	0.516	0.511	0.511	0.124	0.124	0.125	3,663.95	4,697.33	232.29	297.81	1.00	0.97	3.52	466,532.00	8.13	Good Break
CF13-45	CF-ABS	0.517	0.515	0.514	0.123	0.122	0.122	3,850.23	5,007.06	241.41	313.94	1.00	0.97	3.95	502,189.00	8.24	Good Break
CF14-45	CF-ABS	0.514	0.514	0.513	0.123	0.123	0.124	3,859.30	4,924.28	243.52	310.72	1.00	0.97	3.60	494,551.00	8.26	Good Break
CF15-45	CF-ABS	0.515	0.512	0.512	0.124	0.124	0.124	3,793.58	4,664.81	240.89	296.22	1.00	0.97	2.84	459,174.00	8.24	Good Break
CF1-60	CF-ABS	0.516	0.515	0.515	0.124	0.123	0.123	3,005.02	3,719.41	190.52	235.81	1.00	0.97	3.96	405,845.00	8.12	Good Break
CF2-60	CF-ABS	0.515	0.516	0.516	0.125	0.123	0.123	3,039.97	3,747.37	192.73	237.58	1.00	0.97	3.94	400,088.00	8.13	Good Break
CF3-60	CF-ABS	0.516	0.514	0.514	0.124	0.123	0.124	3,172.54	3,866.28	200.50	244.35	1.00	0.97	3.46	438,703.00	8.16	Good Break
CF4-60	CF-ABS	0.515	0.516	0.515	0.123	0.122	0.122	3,137.94	3,867.15	197.06	242.86	1.00	0.97	3.23	394,972.00	8.17	Good Break
CF5-60	CF-ABS	0.514	0.515	0.515	0.122	0.122	0.123	3,061.96	3,751.89	192.29	235.62	1.00	0.97	2.91	397,471.00	8.06	Good Break
CF6-60	CF-ABS	0.515	0.515	0.515	0.123	0.122	0.123	3,188.51	3,866.21	200.24	242.80	1.00	0.96	2.89	399,832.00	8.14	Good Break
CF7-60	CF-ABS	0.515	0.514	0.514	0.123	0.122	0.122	3,180.87	3,881.56	199.44	243.37	1.00	0.98	3.19	418,414.00	8.1	Good Break
CF8-60	CF-ABS	0.514	0.512	0.513	0.125	0.123	0.124	3,070.06	3,811.26	193.41	240.11	1.00	0.97	3.19	401,868.00	8.12	Good Break

Appendix-H: Record-Keeping

CF9-60	CF-ABS	0.515	0.515	0.515	0.123	0.123	0.123	3,239.65	3,935.87	205.39	249.53	1.00	0.97	2.99	406,525.00	8.18	Good Break
CF10-60	CF-ABS	0.517	0.515	0.514	0.123	0.122	0.122	3,167.91	3,922.56	198.63	245.94	1.00	0.97	3.95	402,817.00	8.17	Good Break
CF11-60	CF-ABS	0.517	0.516	0.516	0.122	0.122	0.123	3,214.50	4,013.62	202.51	252.86	1.00	0.97	4.47	417,283.00	8.1	Good Break
CF12-60	CF-ABS	0.516	0.514	0.514	0.124	0.122	0.123	3,153.07	3,924.68	197.70	246.08	1.01	0.97	3.32	419,540.00	8.21	Good Break
CF13-60	CF-ABS	0.517	0.518	0.518	0.118	0.118	0.119	3,529.61	4,405.06	215.31	268.71	1.00	0.97	3.96	444,903.00	8.02	Good Break
CF14-60	CF-ABS	0.514	0.514	0.513	0.123	0.123	0.124	3,222.51	3,988.76	203.34	251.69	1.00	0.97	3.16	409,063.00	8.15	Good Break
CF15-60	CF-ABS	0.518	0.516	0.515	0.123	0.123	0.124	3,192.82	3,893.93	202.42	246.88	1.00	0.97	3.81	428,642.00	8.15	Good Break
CF1-75	CF-ABS	0.517	0.518	0.517	0.124	0.123	0.123	2,857.37	3,399.49	181.73	216.21	1.00	0.97	2.68	384,190.00	8.09	Good Break
CF2-75	CF-ABS	0.518	0.518	0.518	0.124	0.123	0.122	3,020.14	3,612.67	190.87	228.32	1.00	0.97	3.00	391,869.00	8.11	Good Break
CF3-75	CF-ABS	0.519	0.519	0.518	0.122	0.121	0.121	3,241.66	3,914.08	203.25	245.41	1.00	0.97	3.43	409,508.00	8.14	Good Break
CF4-75	CF-ABS	0.517	0.517	0.517	0.125	0.124	0.123	3,176.74	3,750.68	202.04	238.54	1.00	0.97	2.51	412,594.00	8.26	Good Break
CF5-75	CF-ABS	0.518	0.518	0.519	0.122	0.122	0.121	3,170.51	3,817.71	198.79	239.37	1.00	0.97	3.24	436,063.00	8.15	Good Break
CF6-75	CF-ABS	0.517	0.518	0.517	0.122	0.121	0.122	2,929.21	3,349.73	183.37	209.69	1.00	0.96	2.11	402,433.00	8.15	Good Break
CF7-75	CF-ABS	0.518	0.518	0.517	0.121	0.122	0.123	2,951.86	3,511.14	184.79	219.80	1.00	0.96	2.50	407,061.00	8.2	Good Break
CF8-75	CF-ABS	0.518	0.516	0.516	0.122	0.123	0.123	2,938.75	3,471.26	185.14	218.69	1.00	0.96	2.41	409,469.00	8.15	Good Break
CF9-75	CF-ABS	0.518	0.517	0.518	0.121	0.122	0.121	2,907.26	3,279.64	181.99	205.31	1.00	0.96	2.14	387,838.00	8.11	Good Break
CF10-75	CF-ABS	0.517	0.517	0.518	0.124	0.123	0.122	3,096.09	3,636.42	195.36	229.46	1.00	0.97	2.62	418,449.00	8.12	Good Break
CF11-75	CF-ABS	0.516	0.515	0.515	0.124	0.124	0.122	3,094.89	3,659.21	194.36	229.80	1.00	0.97	2.48	417,235.00	8.2	Good Break
CF12-75	CF-ABS	0.518	0.516	0.517	0.123	0.123	0.123	3,109.63	3,700.99	197.46	235.01	1.00	0.96	3.17	430,553.00	8.21	Good Break
CF13-75	CF-ABS	0.518	0.517	0.517	0.122	0.122	0.123	3,165.63	3,797.96	199.75	239.65	1.00	0.97	2.95	408,568.00	8.22	Good Break
CF14-75	CF-ABS	0.518	0.517	0.517	0.122	0.122	0.123	3,064.72	3,629.17	193.38	229.00	1.00	0.96	2.43	427,769.00	8.19	Good Break
CF15-75	CF-ABS	0.518	0.517	0.517	0.123	0.122	0.122	2,955.63	3,273.78	186.50	206.58	1.00	0.97	1.89	389,038.00	8.16	Good Break
CF1-90	CF-ABS	0.516	0.516	0.517	0.123	0.122	0.122	4,203.99	4,268.03	268.64	272.73	0.79	0.76	0.81	653,749.00	8.24	Good Break
CF2-90	CF-ABS	0.516	0.515	0.515	0.122	0.122	0.122	4,515.21	4,561.08	283.56	286.44	0.84	0.82	0.87	677,950.00	8.26	Good Break
CF3-90	CF-ABS	0.515	0.515	0.515	0.124	0.123	0.122	4,250.58	4,335.02	266.94	272.24	0.77	0.74	0.80	692,418.00	8.21	Good Break
CF4-90	CF-ABS	0.513	0.513	0.512	0.124	0.124	0.123	4,237.55	4,295.94	266.97	270.64	0.82	0.79	0.84	652,507.00	8.2	Good Break
CF5-90	CF-ABS	0.515	0.514	0.514	0.123	0.122	0.122	4,158.64	4,219.66	260.75	264.57	0.76	0.74	0.79	658,478.00	8.26	Good Break
CF6-90	CF-ABS	0.512	0.512	0.513	0.124	0.123	0.123	4,295.00	4,347.29	270.58	273.88	0.81	0.79	0.84	669,645.00	8.19	Good Break
CF7-90	CF-ABS	0.513	0.513	0.513	0.123	0.123	0.122	4,297.32	4,339.00	271.16	273.79	0.81	0.79	0.83	665,096.00	8.23	Good Break
CF8-90	CF-ABS	0.513	0.513	0.513	0.124	0.123	0.124	4,309.26	4,344.38	271.91	274.13	0.82	0.81	0.69	682,009.00	8.16	Good Break
CF9-90	CF-ABS	0.512	0.511	0.511	0.123	0.123	0.124	4,305.12	4,353.26	270.79	273.82	0.65	0.63	0.67	624,934.00	8.18	Good Break
CF10-90	CF-ABS	0.514	0.515	0.515	0.122	0.122	0.122	4,360.55	4,416.39	273.41	276.91	0.85	0.82	0.87	606,756.00	8.16	Good Break
CF11-90	CF-ABS	0.519	0.516	0.517	0.122	0.123	0.122	4,220.43	4,257.25	265.89	268.21	0.79	0.76	0.81	650,660.00	8.05	Good Break
CF12-90	CF-ABS	0.518	0.514	0.516	0.122	0.122	0.122	4,399.19	4,450.32	275.83	279.03	0.82	0.79	0.85	672,028.00	8.18	Good Break
CF13-90	CF-ABS	0.517	0.516	0.517	0.123	0.123	0.122	4,358.19	4,398.90	276.75	279.33	0.87	0.85	0.90	620,930.00	8.18	Good Break
CF14-90	CF-ABS	0.518	0.515	0.515	0.124	0.123	0.123	4,303.32	4,359.24	272.83	276.38	0.84	0.81	0.87	671,380.00	8.2	Good Break
CF15-90	CF-ABS	0.514	0.513	0.514	0.124	0.122	0.122	4,286.10	4,363.03	268.31	273.13	0.83	0.80	0.87	651,533.00	8.18	Good Break

Appendix-I: Code Book for Record Keeping

Variable	Name	Description	Code	Value Range	Scale of Measurement	Descriptive Statistics
1	ABS Bone Sample	15 ASTM D638 type I bone samples per level (6 levels)	A1 0/90 through A90 - 75/75	1-90 & 0/90, -15/15, -30/30, -45/45, -60/60, and -75/75 degrees	Nominal	Central Tendency - Mean
2	CFR ABS Bone Sample	15 ASTM D638 type I bone samples per level (6 levels)	CF1 0/90 through CF90 - 75/75	1-90 & 0/90, -15/15, -30/30, -45/45, -60/60, and -75/75 degrees	Nominal	Central Tendency - Mean
3	Bone Width	Sample width in necked down region	W1, W2, W3	13mm ±.5mm	Nominal	Central Tendency - Mean
4	Bone Thickness	Sample thickness is necked down region	T1, T2, T3	3.2mm ± .4mm	Nominal	Central Tendency - Mean
5	Problems in Tensile-Test	Problems observed during bone tensile testing	ND	Qualitative	Nominal	Central Tendency - Mean
6	Tensile Strength at Yield	Newtons (pounds-force) / Cross sectional area (square meters)	T Sth Y	0.000-? Pascal's (Psi)	Nominal	Central Tendency - Mean
7	Tensile Strength at Break	Newtons (pounds-force) / Cross sectional area (square meters)	T Sth B	0.000-? Pascals (Psi)	Nominal	Central Tendency - Mean
8	Tensile Strain at Yield	Change in grip (jaws) separation relative to the original grip	T Stn Y	0.000-? Pascals (Psi) & Percentage	Nominal	Central Tendency - Mean

Appendix-I: Code Book for Record Keeping

9	Tensile Strain and at Break	Change in grip (jaws) separation relative to the original grip at the point of breakage. ((Extension / original grip separation length)*100)	T Stn B	0.000-? Pascals (Psi) & Percentage	Nominal	Central Tendency - Mean
10	Percent Tensile Elongation	Extensometer gage length relative to the original specimen gage length	% E	Percentage	Nominal	
11	Percent Elongation at Yield	Reading extension (change in gage length) at the yield point. ((Extension / original gage length)*100)	% E Y	Percentage	Nominal	Central Tendency - Mean
12	Percent Elongation at Break	Reading extension (change in gage length) at the point of breakage. ((Extension / original gage length)*100)	% E B	Percentage	Nominal	Central Tendency - Mean
13	Modulus of Elasticity	Linear potion of load curve / difference in stress	M	0.000-? Pascals (Psi)	Nominal	Central Tendency - Mean
14	Mass	Mass of the tensile-testing specimen in grams.	Mass	7 to 9 grams	Nominal	Central Tendency - Mean